



WL-TM-92-350-FIBG

AD-A262 482



MODAL SURVEY OF A
FULL-SCALE F-18
WIND TUNNEL MODEL

Levraea, Vincent J.
Henderson, Douglas A.
Pacia, Arnel P.
Banford, Michael P.



Structural Dynamics Branch

SEPTEMBER 1992

Approved for Public Release; Distribution
is Unlimited.

FLIGHT DYNAMICS DIRECTORATE
WRIGHT LABORATORY
WRIGHT-PATTERSON AIR FORCE BASE, OH 4

Reproduced From
Best Available Copy

20001026162

93-06931



632

0001 0000 090

REPORT DOCUMENTATION PAGE			Form Approved OMB No. 0704-0188	
Public reporting burden for this collection of information is estimated to average 1 hour per response, including the time for reviewing instructions, searching existing data sources, gathering and maintaining the data needed, and completing and reviewing the collection of information. Send comments regarding this burden estimate or any other aspect of this collection of information, including suggestions for reducing this burden, to Washington Headquarters Services, Directorate for Information Operations and Reports, 1215 Jefferson Davis Highway, Suite 1204, Arlington, VA 22202-4302, and to the Office of Management and Budget, Paperwork Reduction Project (0704-0188), Washington, DC 20503				
1. AGENCY USE ONLY (Leave blank)	2. REPORT DATE September 1992	3. REPORT TYPE AND DATES COVERED Interim Mar 91 - July 92		
4. TITLE AND SUBTITLE Modal Survey of a Full-Scale F-18 Wind Tunnel Model			5. FUNDING NUMBERS	
6. AUTHOR(S) Vincent J. Levraea Arnel P. Pacia Douglas A. Henderson Michael P. Banford				
7. PERFORMING ORGANIZATION NAME(S) AND ADDRESS(ES) Wright Laboratory WL/FIBG Wright-Patterson AFB OH 45433			8. PERFORMING ORGANIZATION REPORT NUMBER WL-TM-92-350-FIBG	
9. SPONSORING/MONITORING AGENCY NAME(S) AND ADDRESS(ES)			10. SPONSORING/MONITORING AGENCY REPORT NUMBER	
11. SUPPLEMENTARY NOTES				
12a. DISTRIBUTION/AVAILABILITY STATEMENT Approved for public release; distribution unlimited.			12b. DISTRIBUTION CODE	
13. ABSTRACT (Maximum 200 words) The purpose of this investigation was to perform a ground vibration test (GVT) to determine the resonant frequencies, damping, and mode shapes for the F-18 vertical tail structure. This effort represents a subtask of the twin tail buffet work currently studying the buffet response of the F-18 vertical tails to forebody vortices generated at high angles of attack. The GVT was conducted on a full-scale F-18 airframe which had been significantly modified to enable it for use as a full-scale wind tunnel model in the NASA Ames 80 ft x 120 ft wind tunnel facility. Because the major emphasis of the test was to obtain the dynamic characteristics of the vertical tails under tunnel mounting conditions, the GVT was performed with the full-scale model mounted on the tunnel pedestals in the same configuration as would be used for the wind tunnel tests. The primary excitation frequencies of the vortical wake were expected to be below 100 hertz, thus the GVT only measured tail response frequencies below this value. The results give dynamic response information for the first bending, second bending, and first torsional modes of the vertical tails.				
14. SUBJECT TERMS Aircraft Vibration Buffet Tail Buffet Fatigue Resonant Vibration Vibration Testing			15. NUMBER OF PAGES 58	16. PRICE CODE
17. SECURITY CLASSIFICATION OF REPORT UNC	18. SECURITY CLASSIFICATION OF THIS PAGE UNC	19. SECURITY CLASSIFICATION OF ABSTRACT UNC	20. LIMITATION OF ABSTRACT UL	

PREFACE

This report describes the modal vibration survey and parameter estimation of the F-18 airframe vertical tails between March 1991 and July 1992. The survey was conducted by the Structural Dynamics Branch, Flight Dynamics Directorate, Wright Laboratory, Wright-Patterson Air Force Base, under job order number 24010446 entitled, "Twin Tail Buffet." The authors wish to acknowledge the contributions by the technicians and engineers at NASA Ames 80' x 120' facility. Their support led to the successful completion of this project.

Prepared By:

Vincent J. Levraea

Vincent J. Levraea, Captain, USAF
Project Leader
Acoustics and Sonic Fatigue Section

Douglas A. Henderson

Douglas A. Henderson
Aerospace Engineer
Vibration Section

Coordination:

Ralph M. Shimovetz

Ralph M. Shimovetz, Tech Manager
Acoustics and Sonic Fatigue Section

This report has been reviewed and is approved.

Jerome Pearson

Jerome Pearson, Chief
Structural Dynamics Branch
Structures Division

DTIC QUALITY INSPECTED

Accession For	
NTIS GRA&I	<input checked="" type="checkbox"/>
DTIC TAB	<input type="checkbox"/>
Unannounced	<input type="checkbox"/>
Justification	
By _____	
Distribution/	
Availability Codes	
Dist	Avail and/or Special
A-1	

CONTENTS

SECTION	PAGE
I. INTRODUCTION	1
II. TEST SETUP	6
A. AIRCRAFT	6
B. FORCE INPUT SYSTEM	10
C. INSTRUMENTATION	11
D. DATA ACQUISITION EQUIPMENT	17
III. GROUND VIBRATION TEST	20
IV. DATA ANALYSIS	25
V. DISCUSSION OF RESULTS	27
VI. CONCLUSIONS	53
REFERENCES	55

LIST OF FIGURES

FIGURE	TITLE	PAGE
1	F-18 Aircraft	2
2	Vortex Generated by F-18 Leading Edge Extension	3
3	F-18 Airframe in the Ames Tunnel	4
4	Front Tunnel Support Structure	7
5	Truss Structure Used to Mount Rear of Model to Tunnel Pedestal	8
6	Full-Scale F-18 Wind Tunnel Model Mounted in the Ames 80'x 120' Facility	9
7	Shaker Support Rigging	11
8	Close-up of Shaker Support Rigging	11
9	Shaker Attachment Hardware	11
10	Close-up of Shaker Attachment Hardware	11
11	Ground Vibration Test Set-up	11
12	Data Acquisition Equipment	11
13	GVT Set-up for 45.5 Pitch Angle	21
14	Vertical Tail Accelerometer Layout	21
15	Additional Airframe Accelerometer Locations	21
16	Typical Comparison of Test and Estimated Frequency Response Fraction	21
17	Mode Shapes for Vertical Tail First Bending at 28.8 Angle of Attack ..	21
18	Mode Shape for Vertical Tail First Torsion at 28.8 Angle of Attack ..	21
19	Mode Shape for Vertical Tail Second Bending 28.8 Angle of Attack ..	21

I. INTRODUCTION

The need to operate modern fighter aircraft at high angles of attack has led to numerous investigations into the empennage buffet phenomenon. Vortical wakes generated by the aircraft forebody contain large buffeting pressures which impinge on the tail structure. Excessive dynamic response of the tail results, causing damaging vibration. Twin vertical tail aircraft are particularly susceptible to tail buffet. The F-18, shown in Figure 1, is one such twin tail aircraft which has experienced serious tail buffet at high angles of attack. Figure 2 shows the generated vortex trailing aft over the top of the aircraft wing.

To gain a better understanding of the tail buffet phenomenon, Wright Laboratory, NASA Ames Research Center, and the Aeronautical Research Laboratory (ARL) in Australia are involved in a cooperative investigation which is centered around the F-18 airframe. The F-18 was selected because of the availability of a retired airframe and because of the vast database of sub-scale wind tunnel results. To properly understand and predict the structural response of the F-18 vertical tails, the modal characteristics of the tail must be known. Therefore, a ground vibration test (GVT) was performed on the F-18 airframe. This GVT concentrated on the response of the vertical tails. Unique aspects of this test were that the engines had been removed from the aircraft, which substantially reduced the mass of the tail section, and that the GVT was performed with the F-18 mounted on the pedestals of the 80' x 120' wind tunnel at Ames Research Center, as shown in Figure 3. In preparation for the GVT of the F-18 mounted on the tunnel pedestals, a preliminary GVT was conducted with the F-18



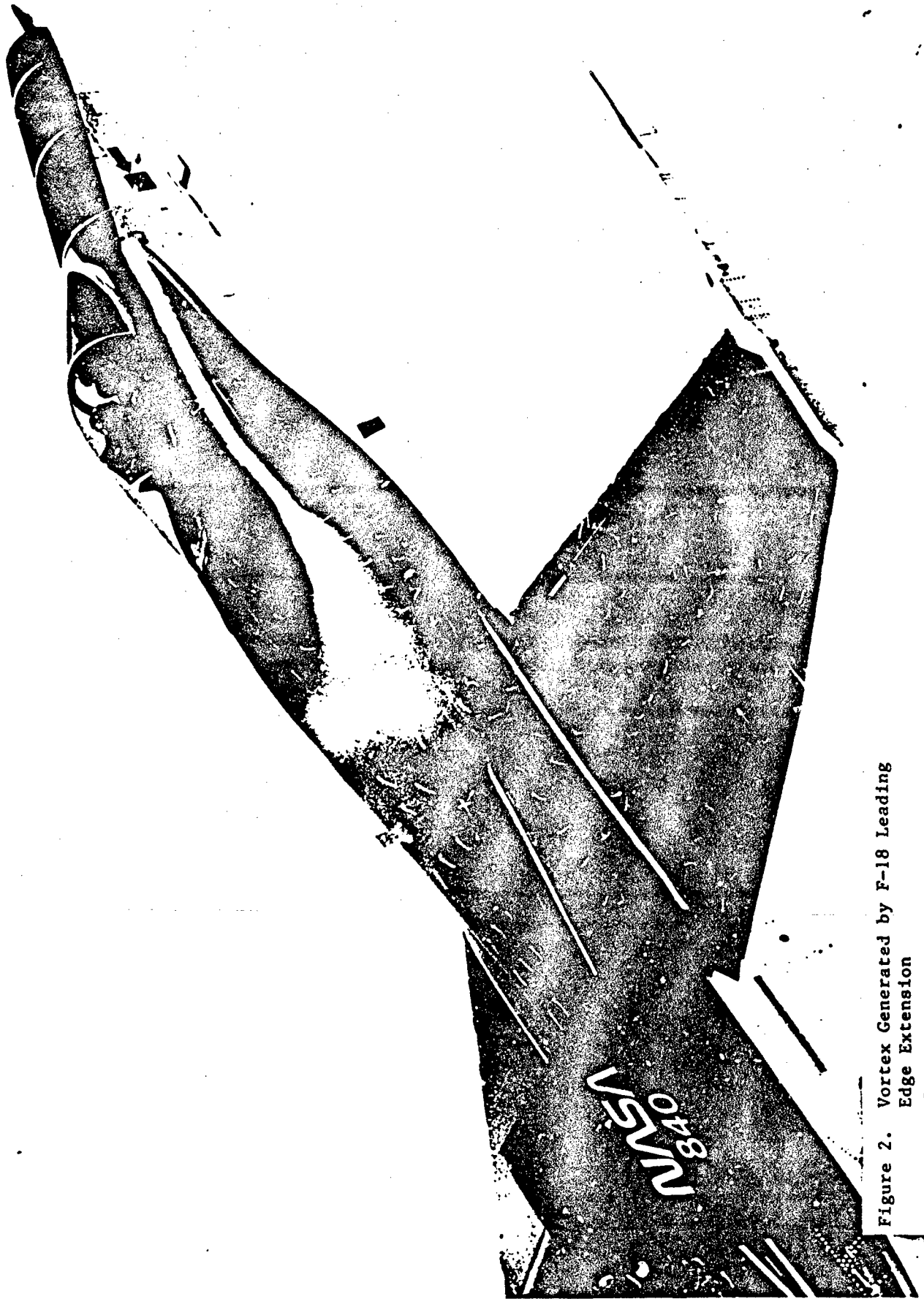


Figure 2. Vortex Generated by F-18 Leading
Edge Extension

mounted on jacks. This GVT served to establish a test procedure and to identify a location at which the applied input force would excite all modes of interest. The results from the preliminary GVT were consistent with the results of the subject GVT and will not be discussed further.

The objective of the F-18 vertical tail modal survey was to estimate the resonant frequencies, damping, and mode shapes for the vertical tail structure up to 100 hertz (Hz). The range of interest was limited because the primary excitation frequencies of the vortical wake are expected to be below 100 Hz. The information gathered will be used for future wind tunnel test planning and validation of computational fluid dynamics (CFD) codes.

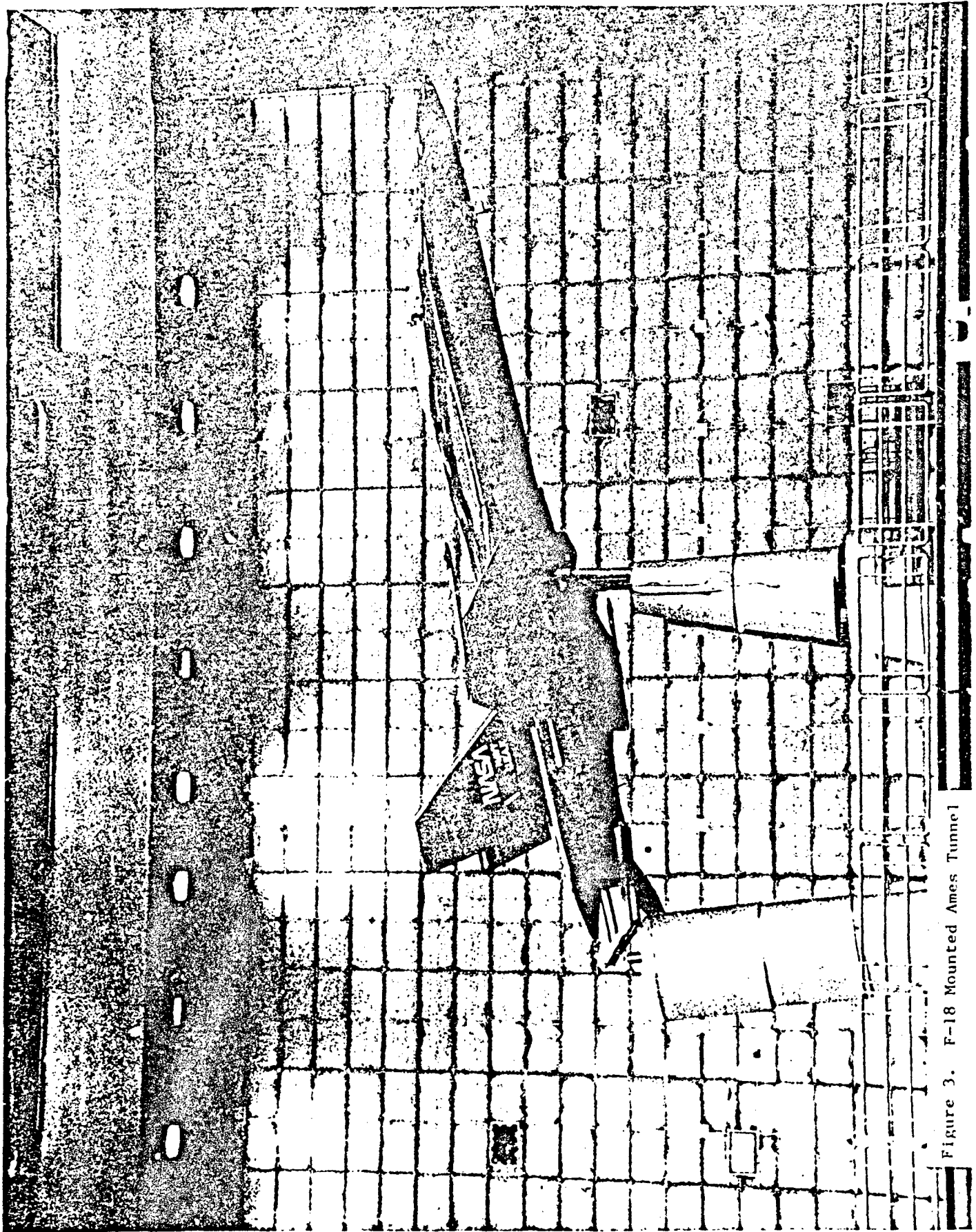


Figure 3. F-18 Mounted Ames Tunnel

II. TEST SETUP

A. AIRCRAFT

The subject investigation was centered around the F-18 airframe. The aircraft, hereafter referred to as the model to avoid confusion with a flight worthy F-18, had been previously retired from active service and acquired by NASA Ames from the United States Navy. Although the primary structure of the airframe was in tact, the model tested represented only the shell of an operational F-18. All the avionics and electronics equipment and both engines were removed from the aircraft. The cockpit was stripped and all fuel and fuel bladders were removed. The main landing gear was replaced by a special support structure, as shown in Figure 4, which served as an adapter to facilitate mounting of the aircraft to the front two tunnel pedestals. The truss structure shown in Figure 5 was attached to engine mounts on each side of the model and to the tail hook hard point. The free end of the truss structure was then attached to the rear pedestal, serving as the rear attachment point of the model.

The model was mounted 35 feet above the tunnel floor on the wind tunnel support pedestals in the 80' x 120' wind tunnel facility at Ames Research Center as shown in Figure 6. During the GVT, the model was configured precisely as required for wind tunnel testing. Except for the horizontal tail actuators, all hydraulic systems on the aircraft were nonfunctional. During the GVT and wind tunnel testing, the horizontal stabilators were set to trim condition values according to the angle of attack under consideration. The trim values had been obtained during previous NASA F-18

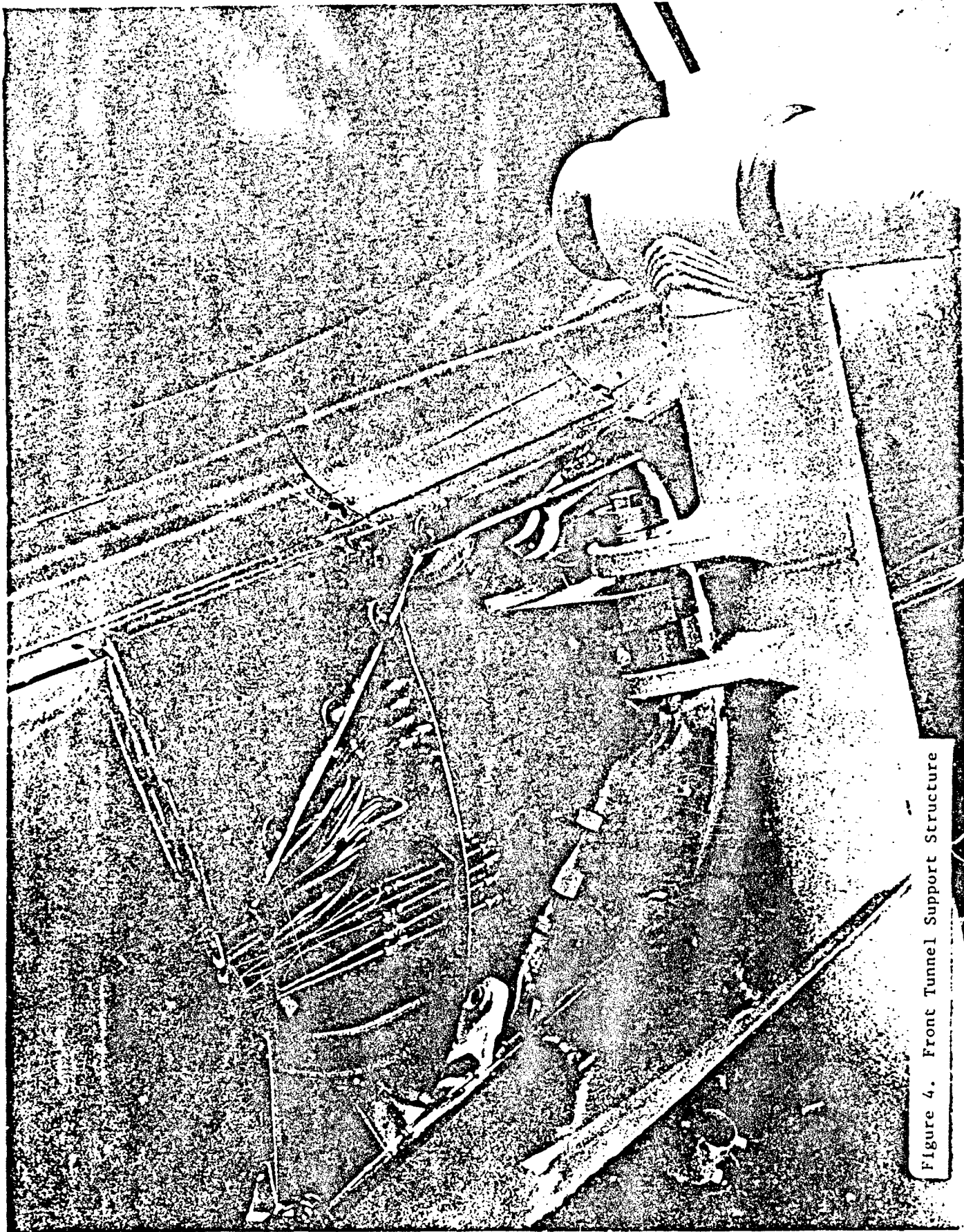
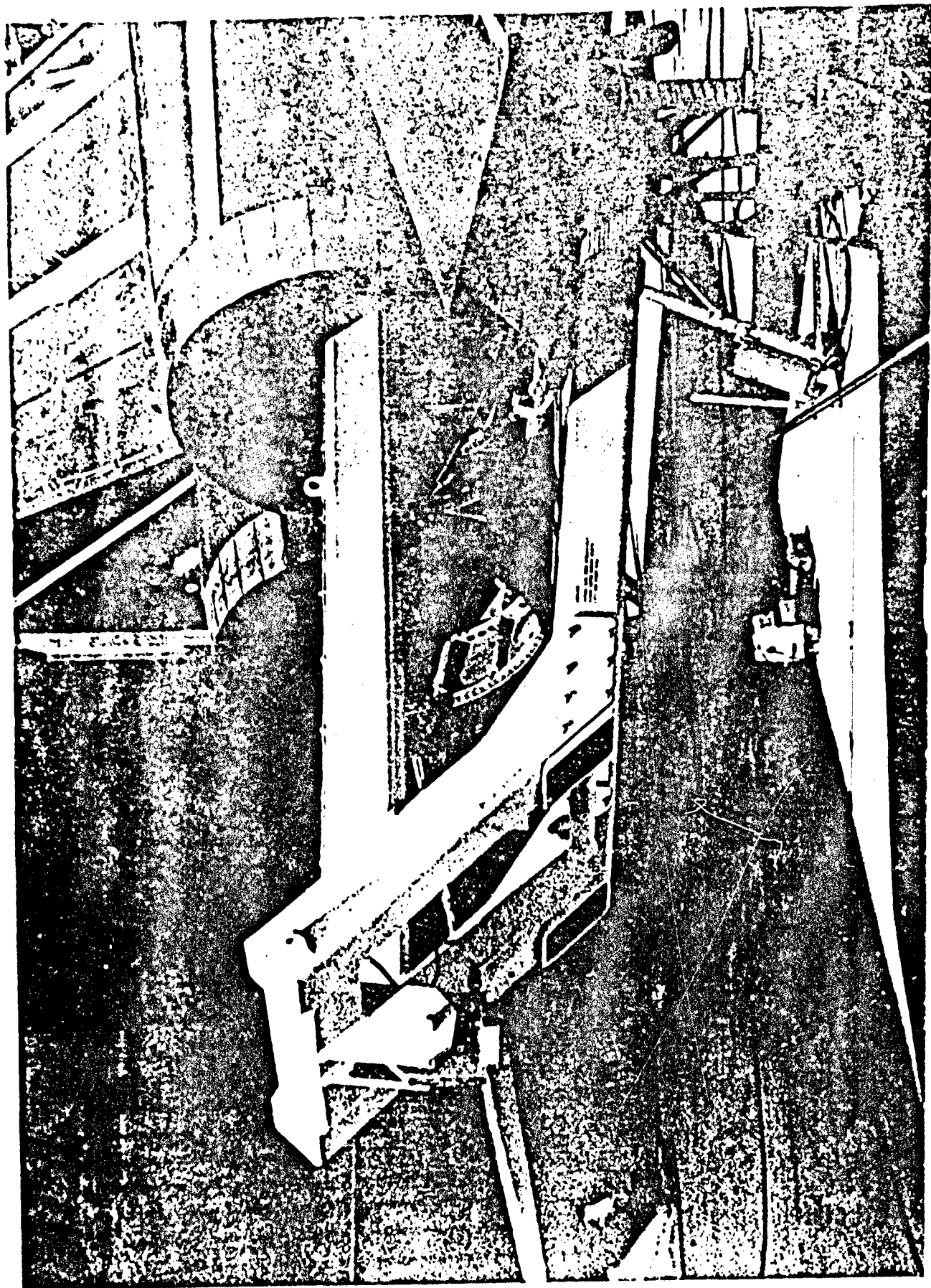


Figure 4. Front Tunnel Support Structure



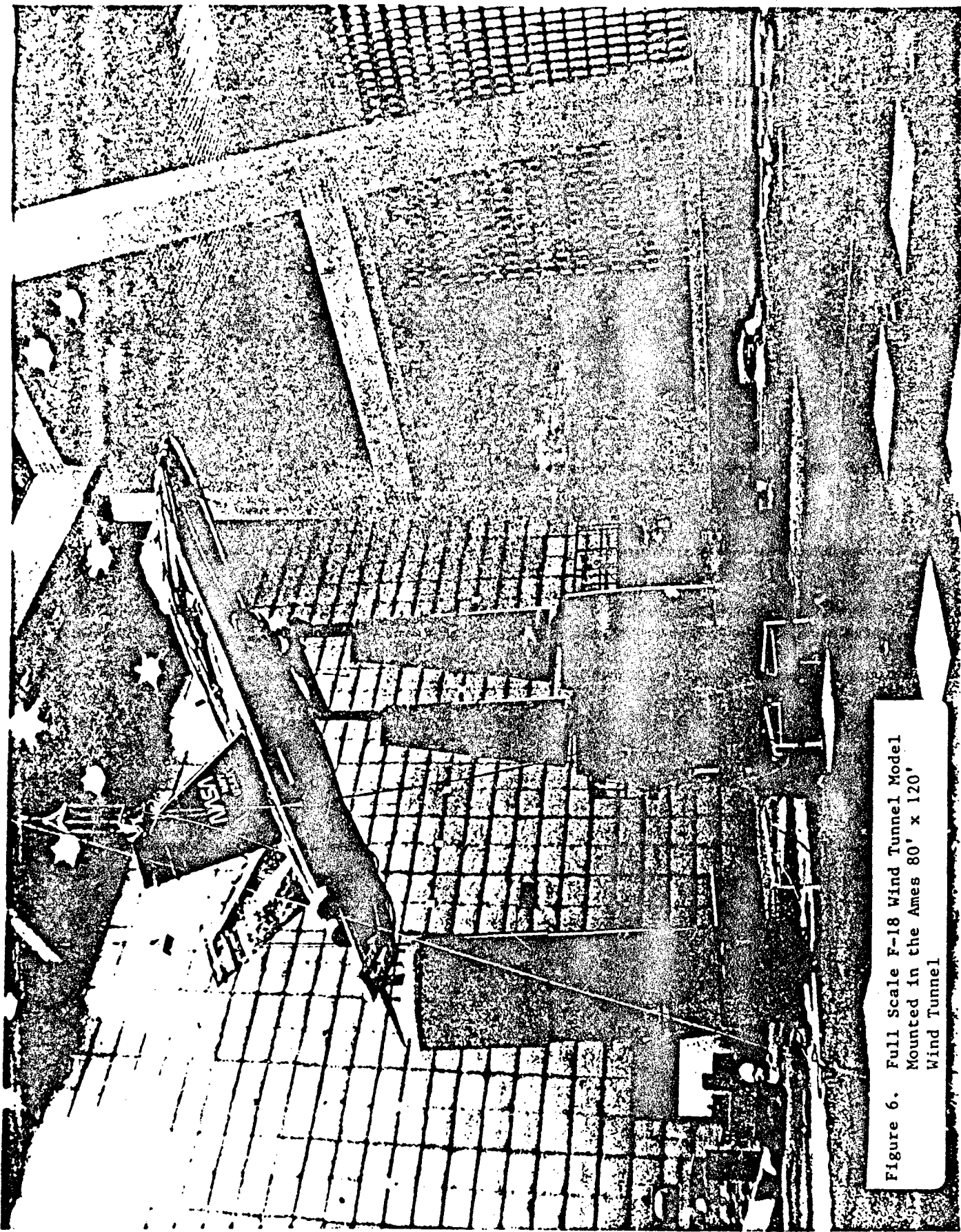


Figure 6. Full Scale F-18 Wind Tunnel Model
Mounted in the Ames 80' x 120'
Wind Tunnel

flight testing. A special link was constructed which replaced the rudder actuator and positioned the rudder at the 0° position in the plane of the vertical tail. After the link was in place, a small amount of movement was still evident in the rudder due to free play in the link attachment points and the rudder hinge. The wing leading edge flaps were held fixed at 33° and the trailing edge flaps and ailerons were held at 0° throughout the GVT and wind tunnel testing.

B. FORCE INPUT SYSTEM

The input force was provided by 2 Unholtz-Dickie Model 4 electromechanical shakers rated at 75 pounds sine and capable of a peak-to-peak stroke of 4 inches. To input enough energy into the vertical tails, a shaker was attached to each tail and the tails excited simultaneously. Each shaker weighed approximately 220 pounds, which provided the necessary reactive mass. Recall that the GVT was performed with the aircraft mounted on the tunnel support pedestals; therefore, a special rigging was used to position the shakers on the vertical tails.

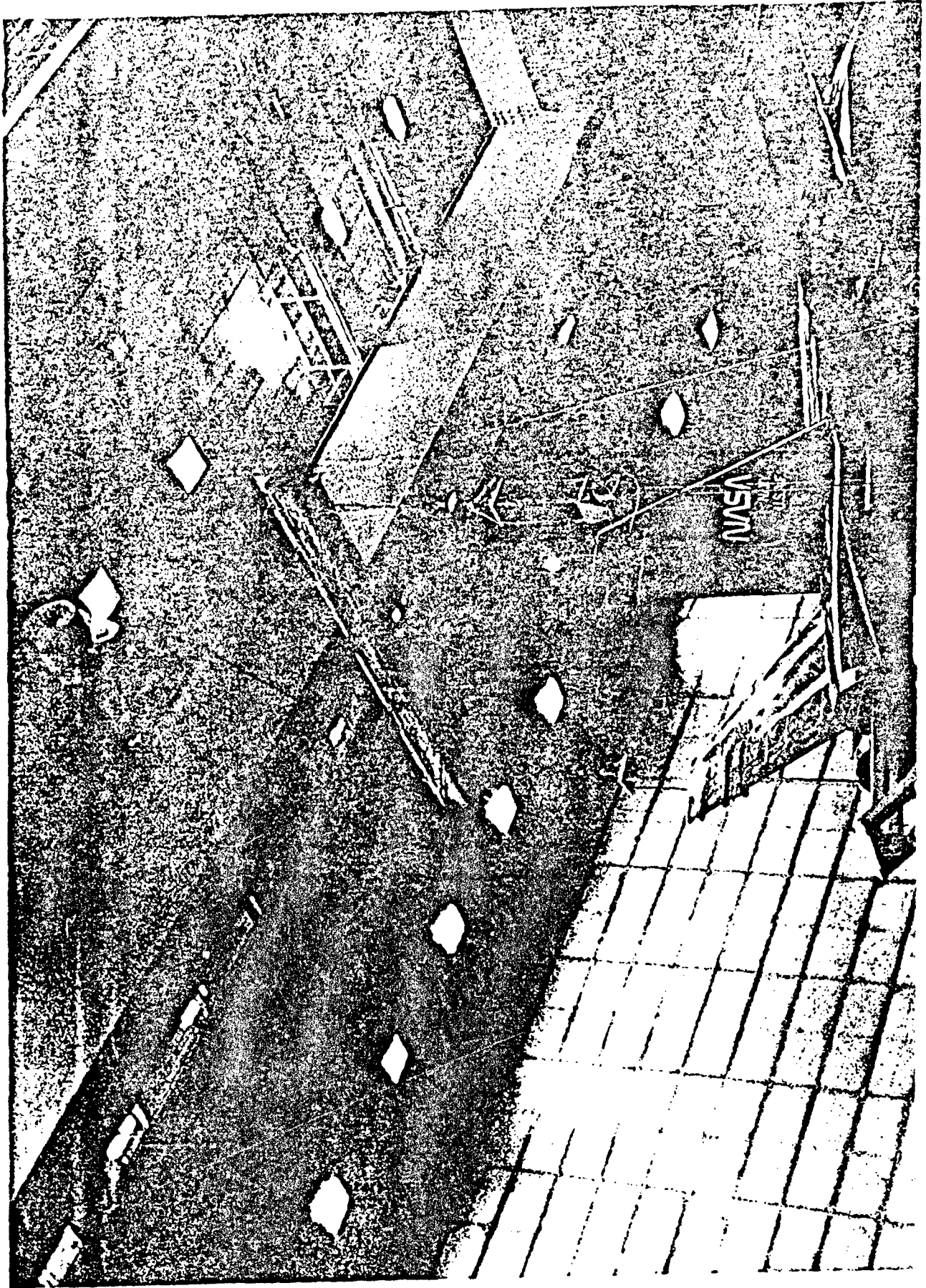
The shakers were suspended from the primary crane in the 80' x 120' tunnel by way of the rigging shown in Figures 7 and 8. The rigging consisted of an 18.5' long, 3070 pound cross-bar attached to the crane hook by cables and held in place by four guy wires. The combination of a heavy cross-bar and guy wire support provided a stable platform from which to hang the shakers. Each shaker was suspended from the cross-bar using a cable, a manual hoist, and a harness designed for direct attachment to the frame of the shaker. The overhead crane was used for gross positioning of the two

shakers, and the manual hoist was used for minor, independent shaker height adjustments.

The shaker armature was connected to the side of the vertical fin using a short stinger, a fixture to compensate for the cant angle of the vertical fin, and a suction cup. A force gauge was installed between the fixture and the suction cup to measure the applied excitation force. This arrangement was used for both shakers, and is shown in Figures 9 and 10. The suction cup was machined out of aluminum and had a rubber O-ring which came into contact with the vertical tail to provide the vacuum seal required and prevent marring of the tail surface. A small portable vacuum pump was used to create the vacuum within the suction cup, securing the shaker to the tail and allowing transmission of the input force. Figure 11 shows a view of both vertical tails with the shakers and associated hardware in place.

C. INSTRUMENTATION

A PCB Model 208A03 force gauge, shown in Figure 10, was used to measure the excitation force input to the vertical tail. This gauge has a sensitivity of 10 mV/lb. PCB Structcel Model 330A accelerometers measured the response of the wind tunnel model. The accelerometers were mounted to the model using hot glue. To maintain the proper orientation of the axes of the reference accelerometers, these accelerometers were mounted on a fixture which compensated for the cant angle of the vertical tail, as shown in Figure 10. The 80' x 120' wind tunnel is open to the outside atmosphere, thus the environment within the tunnel was naturally breezy and cool. There was concern that



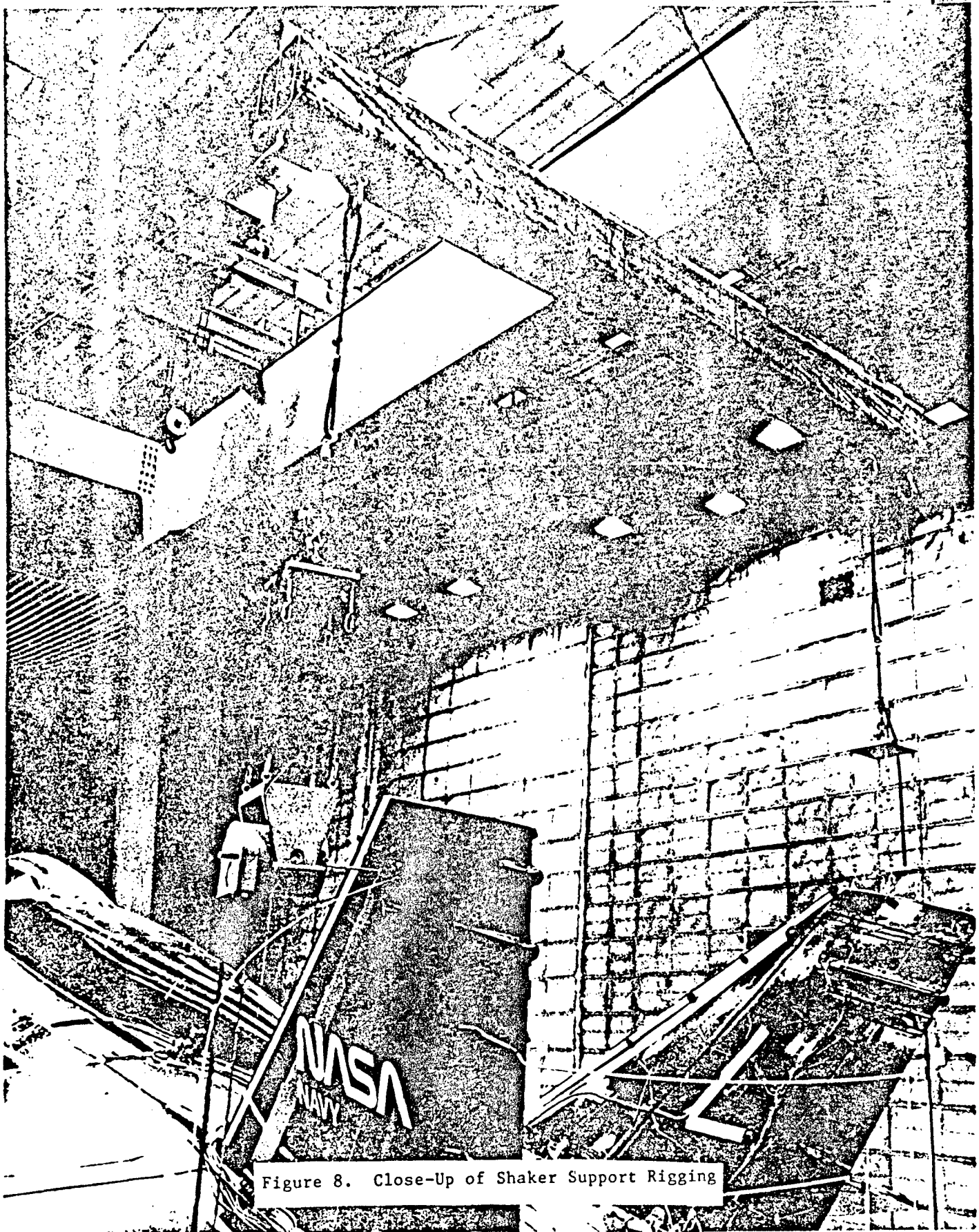
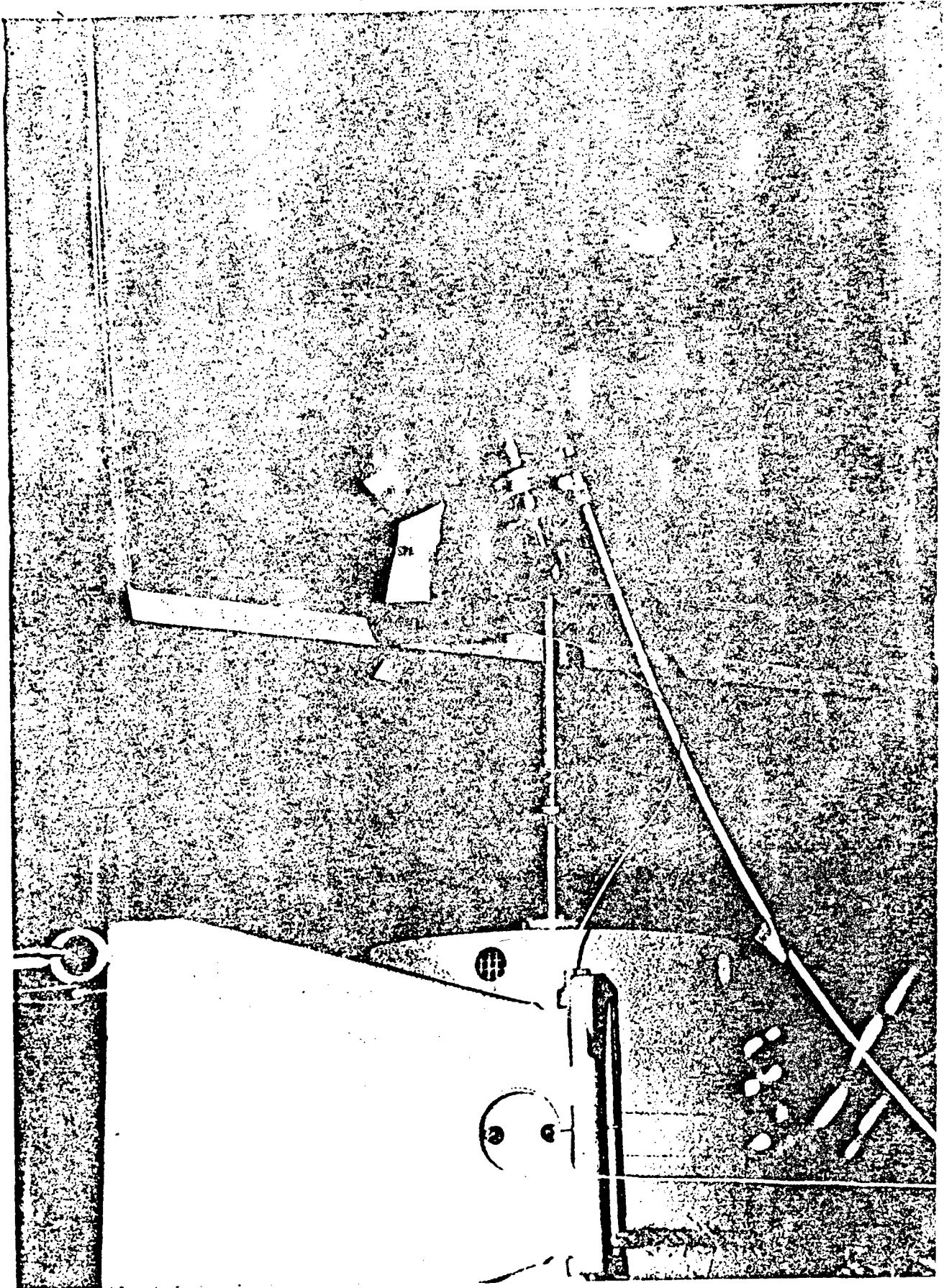


Figure 8. Close-Up of Shaker Support Rigging



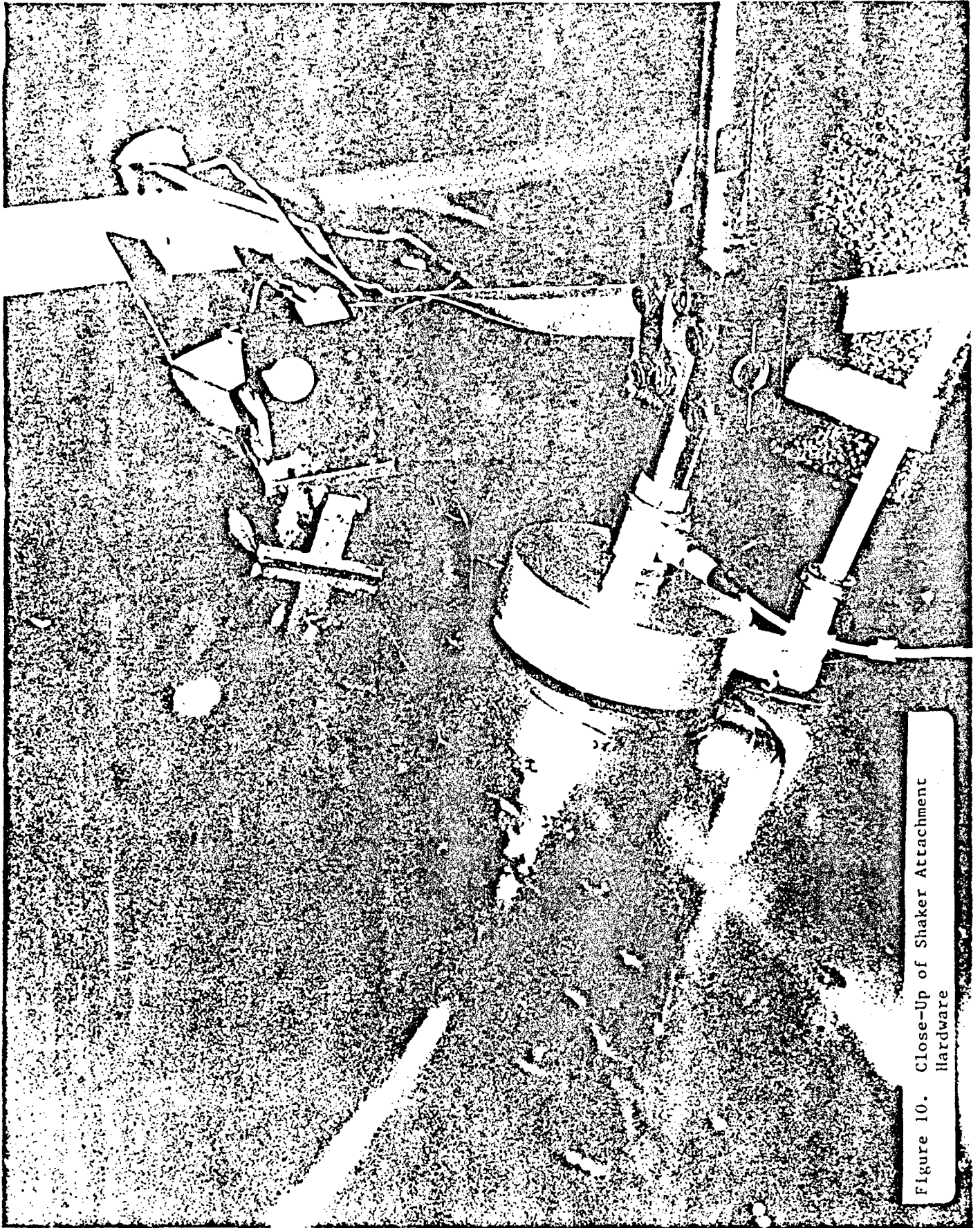


Figure 10. Close-Up of Shaker Attachment Hardware

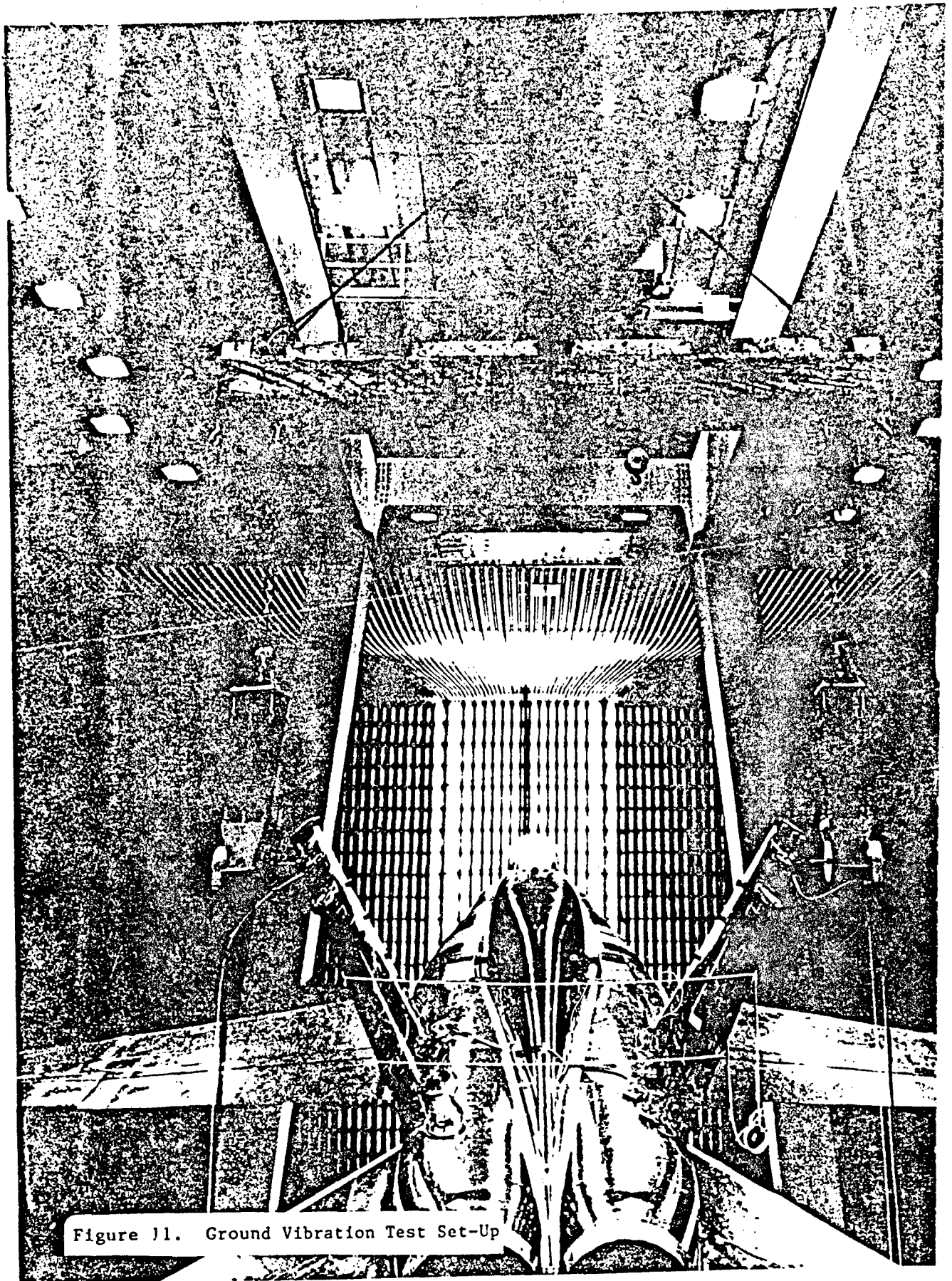


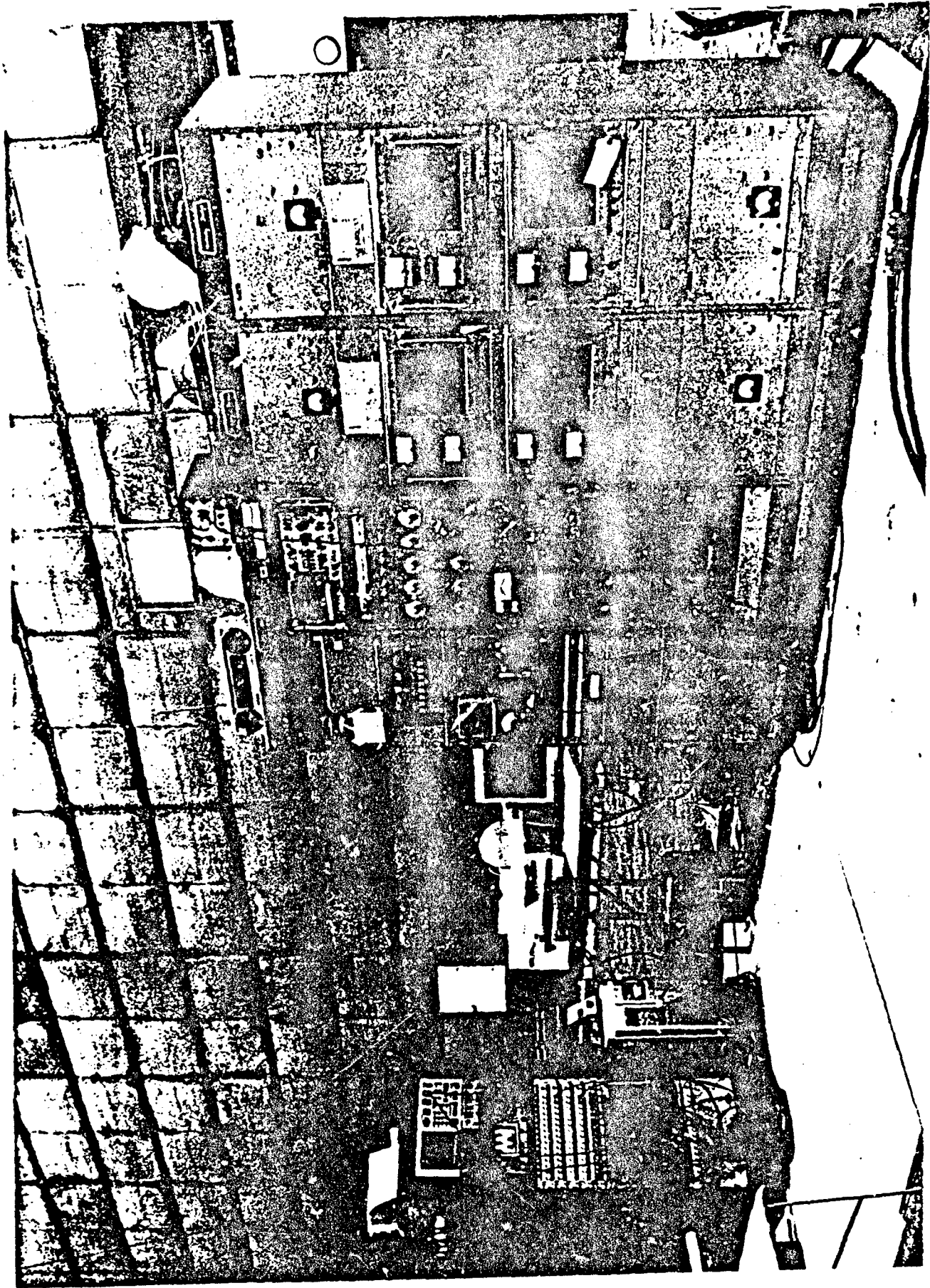
Figure 11. Ground Vibration Test Set-Up

temperature fluctuations would corrupt the data. As a precaution, foam covers, shown in Figure 9, were fabricated and placed over the accelerometers to protect them from the breeze and associated rapid temperature fluctuations.

D. DATA ACQUISITION EQUIPMENT

The data acquisition equipment is shown to the left of the shaker control and field supplies in Figure 12. A rack containing a two-channel spectrum analyzer, a two-channel analog oscilloscope, 7 rack mounted 15 channel accelerometer amplifiers, 4 Intec autogain ranging amplifier cards for the force gauges and a 15 volt DC power supply for the Intec amplifier cards is shown in the left side of the picture. The analog oscilloscope and the two-channel spectrum analyzer were used to troubleshoot the data acquisition system and calibrate accelerometers. The Intec amplifiers were fixed at a gain multiplier of 100.

The data were acquired by a Zonic + AND Corporation System 7000 data acquisition system shown to the right of the equipment rack in Figure 12. The system was able to collect 32 channels of data simultaneously while providing two separate, 0.1 to 150 Hz, uncorrelated random signals to each shaker. The digital signal processor had the capability to automatically adjust amplifier gain range settings in order to optimize the acquisition setup. Ranges up to 10 volts peak could be selected. A Hanning window filter was applied to all of the accelerometer channels, whereas a flat window filter was applied to the force gauge channels. Data were displayed on the computer monitor, shown on the table to the right of the equipment rack, as they were sampled. Sixteen



display windows could be monitored on the screen at one time, but in most cases only four windows were viewed.

III. GROUND VIBRATION TEST

The ground vibration test (GVT) of the full-scale F-18 wind tunnel model was performed with the model mounted in the 80' x 120' wind tunnel at the Ames Research Center. Buffet pressures would be measured at various pitch angles during wind tunnel testing; therefore, it was decided to quantify what, if any, effect pitch angle had on the vertical tail response. The response of the model was measured at three different pitch angles. The pitch angles selected were 16°, 28.8°, and 45.5°. These values of pitch angle were selected to give a sufficient range in pitch angle. Figure 13 shows the test set-up for the 45.5° pitch angle.

Excitation was provided by two 75 pound shakers, one driving each of the vertical tails, to input enough energy into the aircraft empennage structure; the responses of the vertical tails were the primary objective of the test. The shaker attachment for each vertical tail was at the 30% chord and 87% span intersection. This location was selected before testing and was based on the preliminary GVT test results which showed that the three primary modes of interest, namely first bending, first torsion, and second bending, would be excited at this location. These same attachment points were used for each of the three pitch angles investigated.

The response measurements of the wind tunnel model were taken at various airframe locations, with primary emphasis on the vertical tails. Eighty six accelerometer locations were used for the GVT, with 48 test locations and 6 reference accelerometers located on the two vertical tails. The 6 reference accelerometers were arranged in 2 tri-axial groups located near the force inputs. A sketch of the accelerometer grid used for



Figure 13. GVT Set-Up For 45.5° Pitch Angle

each tail is presented in Figure 14. These grid locations were chosen based on past vertical tail GVT results. The remaining 32 accelerometers were located on the model as follows: a tri-axial group was located on each side of the forward fuselage just in front of the canopy, a tri-axial group was located on each side of the model at the intersection of the fuselage and wing near the center of the wing, a tri-axial group was located on each side of the model at the intersection of the vertical tail and the engine bay near the center of the tail, a bi-axial group (measuring x and y accelerations) was located on each of the three tunnel support pedestals near the model attachment points, and two accelerometers were placed at the ends of each wing and horizontal tail to measure response along the z-axis. Figure 15 shows a sketch of the accelerometer locations used for the fuselage, wing, and horizontal stabilators. Figure 15 also shows the reference coordinate system used for acceleration measurements.

VERTICAL TAIL ACCELEROMETER LAYOUT

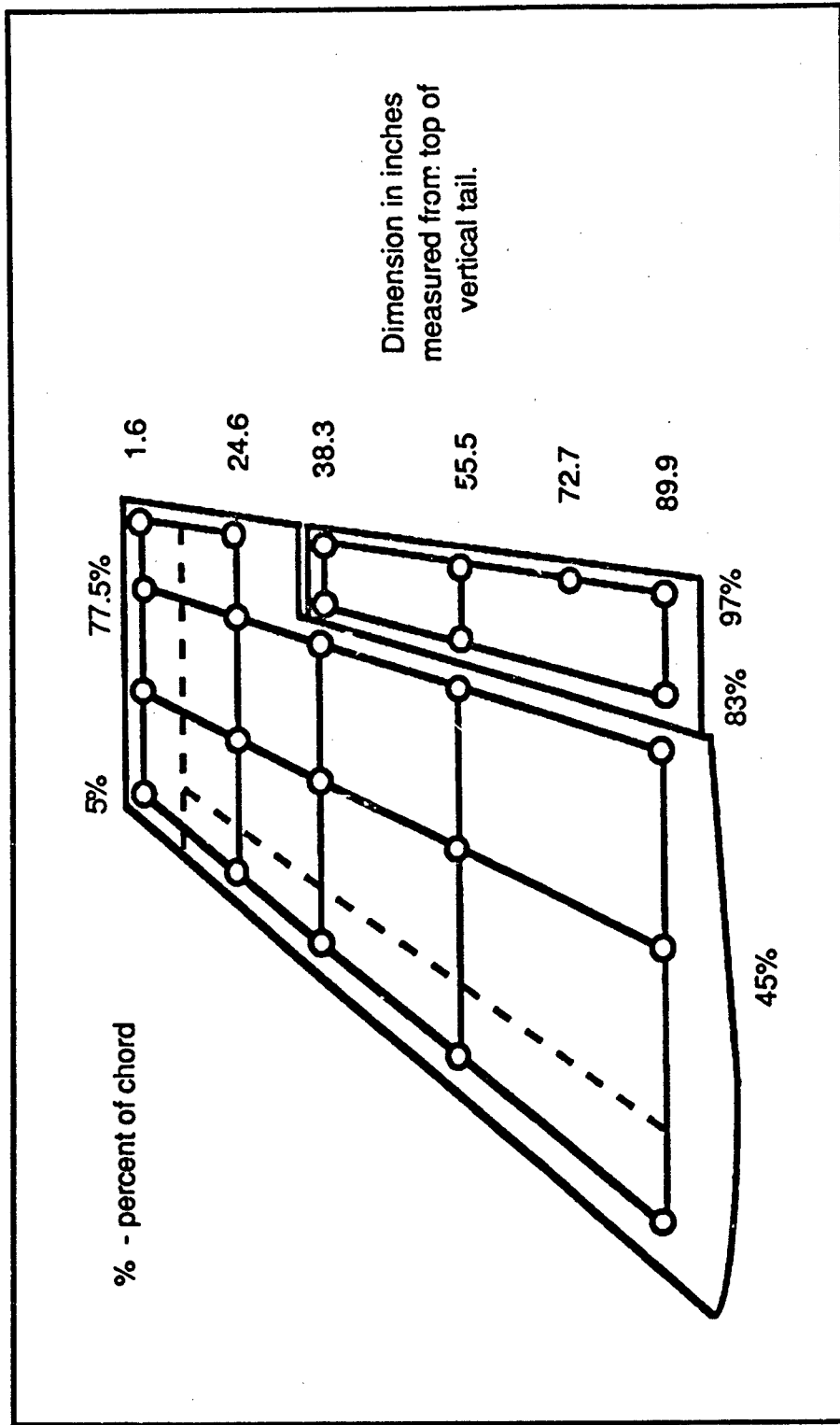


Figure 14. Vertical Tail Accelerometer Layout

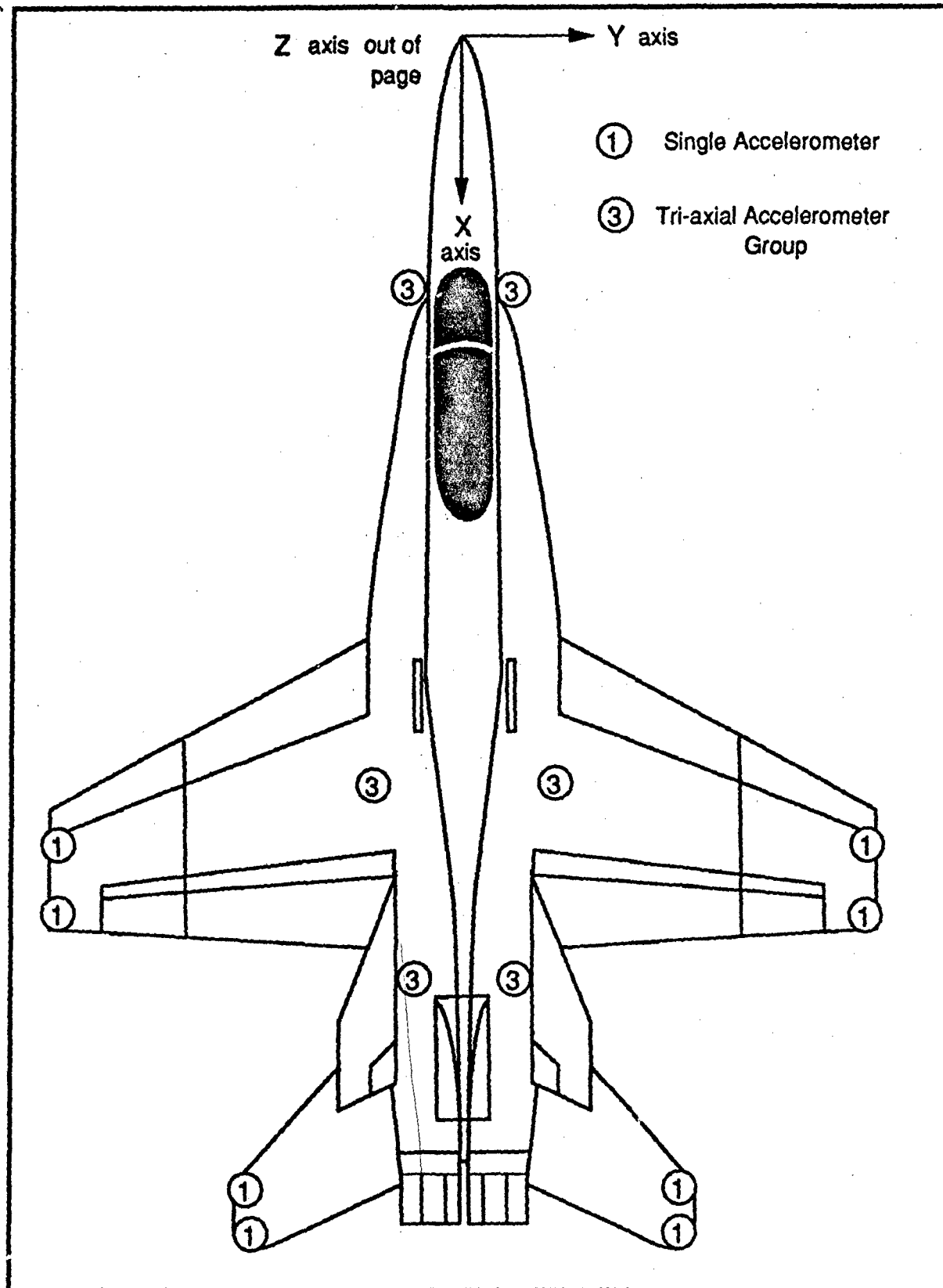


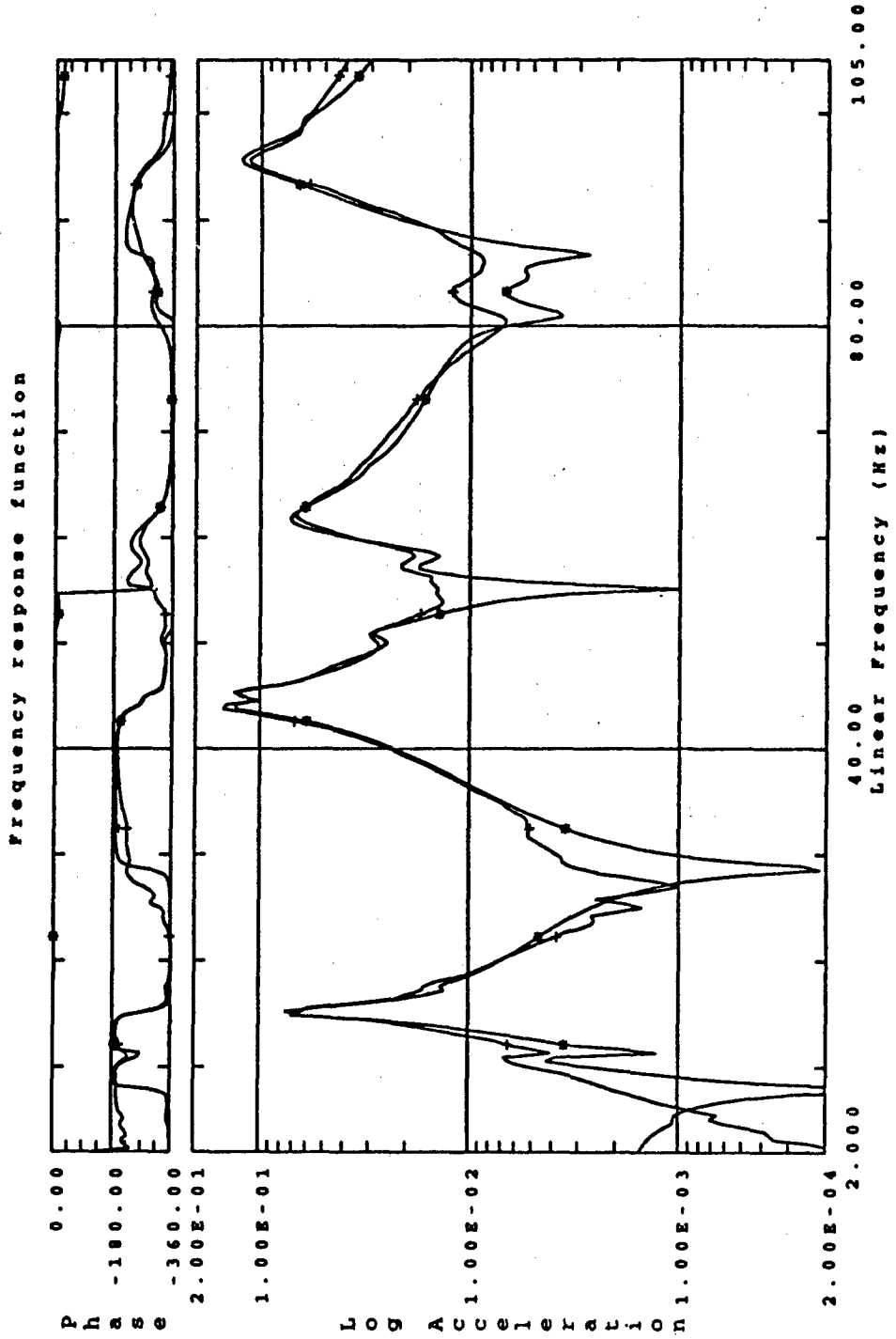
Figure 15. Additional Airframe Accelerometer Locations

IV. DATA ANALYSIS

An initial attempt at analyzing the model data was made estimating the modal frequencies and complex mode shapes of nine model configurations. The nine model configurations consisted of three angle of attack positions, hydraulic power to the stabilators on or off and the use or non-use of bungee to tie down the tail rudders. The purpose of this initial estimate was to determine the effects the addition of bungee, hydraulic pumps, and model angle of attack had on the modal parameters so that a more detailed analysis could focus on the most important set of data. Once those sets of data were selected, a more detailed analysis was performed to identify the modal frequencies, damping ratios and mode shapes.

The modal parameters and mode shapes were estimated by the Structural Dynamics Research Corporation's Test Data Analysis System (TDASTM) software package. The PolyreferenceTM time domain method was used to estimate the six major vertical tail modal frequencies, damping and mode shapes. The PolyreferenceTM method can estimate modal parameters and mode shapes from multi-located shakers exciting the two vertical tails simultaneously. This results in globally estimated modal parameters and mode shapes. As an example, a typical comparison of an estimated frequency response function (FRF) curve and the test FRF data is shown for the 16.0° angle of attack test condition in Figure 16.

13'Aug



V. DISCUSSION OF RESULTS

The initial estimates included only complex modal parameters and mode shapes. This provided an indication of how orthogonal the modes were and what effects the different test conditions had on the modal parameters. The estimated frequencies from this analysis are shown in Table 1. Mode 1 was found to be the model support structure sway frequency. Modes 2 and 3 are the first vertical tail bending modes, antisymmetric and symmetric respectively. They are generally around 15.0 Hz. The first two torsion modes, modes 4 and 5 were found around 45.0 Hz. Mode 4 was found to be symmetric and mode 5 the antisymmetric mode shape. The second bending modes 6 and 7, were found in the 60 Hz range, with mode 6 being the symmetric and mode 7 being the antisymmetric mode shapes.

It is evident from Table 1 that the effects of constraining the tail rudders with bungee and hydraulically powering the horizontal stabilizers did not significantly change the estimated frequencies within each model angle of attack. It was evident that modes 6 and 7 frequencies were not as consistent as the other modal frequencies, showing as high as a 7.5% difference. This indicates that the shakers were not as optimally located for that mode as we would have liked. The other modal frequencies did not differ over 2.0%, and most did not reach 1.0%.

AOA	TEST PARAMETERS	MODE (HZ)						
		1	2	3	4	5	6	7
16.0°	Bungee, Hydraulics Off	11.5	15.2	15.5	44.2	45.4	62.6	62.6
	No Bungee, Hydraulics On	11.6	15.2	15.5	44.2	45.3	57.9	61.5
	No Bungee, Hydraulics Off	11.7	15.3	15.6	44.2	45.3	61.3	61.8
28.8°	Bungee, Hydraulics On	10.7	15.1	15.3	43.9	45.1	60.0	63.2
	No Bungee, Hydraulics On	10.9	15.1	15.3	43.9	45.0	60.6	61.5
	No Bungee, Hydraulics Off	10.9	15.1	15.3	43.9	45.0	61.6	64.9
45.5°	Bungee, Hydraulics On	10.1	15.1	15.8	44.7	45.5	61.0	65.0
	No Bungee, Hydraulics On	10.2	15.1	15.1	44.5	45.3	61.1	63.4
	Bungee, Hydraulics Off	10.2	15.4	15.8	44.7	45.1	63.2	63.8

Table 1. F-18A Initial Parameter Estimation Comparison of Aircraft Test Conditions

Table 1 also shows that the angle of attack had the most effect on the dynamic response of the model. As would be expected, mode 1 had the largest difference of 12.8% because the model support sway mode was directly affected by the variable height of the model support columns. Least affected were modes 4 and 5, the first torsion modes. They differed at most by 2.0%. The first and second bending modes worst case differences were no more than 3.2% and 5.2% respectively.

Once it was determined that the angle of attack had the most effect on the model's dynamics, a detailed analysis was conducted on each of the model angle of attack configurations (16.0°, 28.8° and 45.5°) with hydraulic power on and no bungees attached to the rudders. Modal parameters consisting of frequencies and damping ratios were estimated using a complex estimate. Then the normal mode shapes and generalized mass properties were estimated. These results are shown in Tables 2 and 3. The validity of the modal model was checked using the Modal Assurance Criteria (MAC) on the 16.0° modal parameters, the results of which are shown in Table 4. As can be seen, the off-diagonal terms were below 0.100. This means that the modes were orthogonal and not likely to be correlated with other modes. Since the mode shapes were similar, it was not expected that the MACs for the other modes would be much different.

Further validation was found when comparing the results from a Canadian ground vibration test [4]. These results are included in Table 5. The results were very similar except that the Canadians did not identify the second bending mode near 60 Hz. It appears that the Canadians did not attempt to identify the modes, e.g. first bending, first torsion, etc., and the test may have simply overlooked the mode. If in fact the mode was

AOA (DEG)	FREQUENCY (HZ)	MODAL MASS (LB SEC²/IN)	DAMPING (C/C)	MODAL DESCRIPTION
16.0	15.40	107.665	.025	1st Bending
	44.21	65.794	.012	1st Torsion
	61.32	60.168	.027	2nd Bending
28.8	15.44	55.752	.022	1st Bending
	43.95	31.616	.013	1st Torsion
	61.55	39.288	.028	2nd Bending
45.5	15.64	30.521	.039	1st Bending
	43.92	37.297	.024	1st Torsion
	62.63	1033.273	.005	2nd Bending

Table 2. Symmetric F-18A Modal Parameters

AOA (DEG)	FREQUENCY (HZ)	MODAL MASS (LB SEC²/IN)	DAMPING (C/C)	MODAL DESCRIPTION
16.0	15.30	119.209	.033	1st Bending
	45.38	97.383	.011	1st Torsion
	61.94	307.111	.012	2nd Bending
28.8	15.13	65.864	.021	1st Bending
	45.12	59.930	.012	1st Torsion
	62.19	158.979	.010	2nd Bending
45.5	15.11	55.467	.017	1st Bending
	45.36	51.658	.012	1st Torsion
	63.57	55.936	.022	2nd Bending

Table 3. Antisymmetric F-18A Modal Parameters

1.000	0.111	0.048	0.027	0.094	0.029
0.111	1.000	0.055	0.017	0.009	0.066
0.048	0.055	1.000	0.014	0.001	0.075
0.027	0.017	0.014	1.000	0.008	0.026
0.094	0.009	0.001	0.008	1.000	0.005
0.029	0.066	0.075	0.026	0.005	1.000

Table 4. F-18A Modal Assurance Criteria (MAC) Results, 16.0° AOA

overlooked, it could possibly be due to an inadequate input force location. As was discussed earlier, we experienced a similar problem shown by the inconsistencies in identifying the modal frequency for the second bending mode. Otherwise, the results compared very well.

The modal masses ($\text{lb sec}^2/\text{in}$) are shown in Tables 2 and 3. The modal masses were calculated based on the experimental data and estimated mode shapes given in Tables 6-23. The method described [3] uses the reference and response location eigenvectors, the viscous damping ratio, and the modal frequency and normalizing to the maximum eigenvector.

The mode shapes were generally consistent between the three different aircraft angles of attack tested. A typical set of mode shapes is shown for the 28.8° angle of attack in Figures 17-19. The figures depict the deflected mode shapes of the vertical tails only.

The damping ratio values shown in Tables 2 and 3 remained fairly consistent between test conditions. There were two exceptions to that, at 62.2 Hz, symmetric, 45.5° and at 45.5 Hz, antisymmetric, 28.8° . Both of these damping values significantly dropped from the other similar modes damping values at different angle of attack. Nothing has yet been found to explain the reason why they are different except that the angle of attack may be playing a role in changing the effective boundary condition at the vertical tail and fuselage interface.

<u>MODE</u>	<u>SYMMETRIC</u>		<u>ANTISYMMETRIC</u>	
	FREQUENCY (HZ)	DAMPING (C/C)	FREQUENCY (HZ)	DAMPING (C/C)
Mode 1	15.21	.021	15.23	.019
Mode 2	45.27	.031	45.47	.042
Mode 3	96.75	-----	96.80	-----

Table 5. Canadian Ground Vibration Test Results

LOC	X	Y	Z
1	0.00000E+00	-1.18109E-05	0.00000E+00
2	0.00000E+00	-5.41259E-04	0.00000E+00
3	0.00000E+00	-1.36790E-03	0.00000E+00
4	0.00000E+00	-2.87629E-03	0.00000E+00
5	0.00000E+00	-8.96010E-03	0.00000E+00
6	0.00000E+00	-1.19224E-02	0.00000E+00
7	0.00000E+00	-3.28765E-03	0.00000E+00
8	0.00000E+00	-6.30407E-03	0.00000E+00
9	0.00000E+00	-8.88170E-03	0.00000E+00
10	0.00000E+00	-1.03670E-02	0.00000E+00
11	0.00000E+00	-1.62053E-02	0.00000E+00
12	0.00000E+00	-7.00161E-03	0.00000E+00
13	0.00000E+00	-1.27138E-02	0.00000E+00
14	0.00000E+00	-1.92025E-02	0.00000E+00
15	0.00000E+00	-1.80031E-02	0.00000E+00
16	0.00000E+00	-2.44749E-02	0.00000E+00
17	0.00000E+00	-1.13755E-02	0.00000E+00
18	0.00000E+00	-1.66284E-02	0.00000E+00
19	0.00000E+00	-2.27420E-02	0.00000E+00
20	0.00000E+00	-2.72731E-02	0.00000E+00
21	0.00000E+00	-2.31577E-02	0.00000E+00
22	0.00000E+00	-2.94769E-02	0.00000E+00
23	0.00000E+00	-3.67557E-02	0.00000E+00
24	0.00000E+00	-4.85024E-02	0.00000E+00
25	-9.47614E-03	-1.48530E-02	2.15585E-03
28	0.00000E+00	3.98424E-04	0.00000E+00
29	0.00000E+00	-1.91109E-04	0.00000E+00
30	0.00000E+00	-1.25346E-03	0.00000E+00
31	0.00000E+00	-2.09393E-03	0.00000E+00
32	0.00000E+00	-5.47392E-03	0.00000E+00
33	0.00000E+00	-9.61873E-03	0.00000E+00
34	0.00000E+00	-3.03887E-03	0.00000E+00
35	0.00000E+00	-6.11649E-03	0.00000E+00
36	0.00000E+00	-9.23631E-03	0.00000E+00
37	0.00000E+00	-1.27986E-02	0.00000E+00
38	0.00000E+00	-1.31455E-02	0.00000E+00
39	0.00000E+00	-6.15936E-03	0.00000E+00
40	0.00000E+00	-1.08854E-02	0.00000E+00
41	0.00000E+00	-1.55750E-02	0.00000E+00
42	0.00000E+00	-1.61847E-02	0.00000E+00
43	0.00000E+00	-2.04677E-02	0.00000E+00
44	0.00000E+00	-1.04387E-02	0.00000E+00
45	0.00000E+00	-1.60860E-02	0.00000E+00
46	0.00000E+00	-2.03137E-02	0.00000E+00
47	0.00000E+00	-2.55861E-02	0.00000E+00
48	0.00000E+00	-2.27890E-02	0.00000E+00
49	0.00000E+00	-2.60946E-02	0.00000E+00
50	0.00000E+00	-3.34926E-02	0.00000E+00
51	0.00000E+00	3.48446E-03	0.00000E+00
52	1.46384E-03	-1.85422E-02	-7.22185E-03

Table 6. 15.40 Hz, 16.0° AOA, Symmetric Mode Shape Listing

LOC	X	Y	Z
1	0.00000E+00	-2.01104E-04	0.00000E+00
2	0.00000E+00	-6.86645E-04	0.00000E+00
3	0.00000E+00	-1.52095E-03	0.00000E+00
4	0.00000E+00	-3.34392E-03	0.00000E+00
5	0.00000E+00	-1.14564E-02	0.00000E+00
6	0.00000E+00	-1.40701E-02	0.00000E+00
7	0.00000E+00	-2.88954E-03	0.00000E+00
8	0.00000E+00	-5.40360E-03	0.00000E+00
9	0.00000E+00	-8.97736E-03	0.00000E+00
10	0.00000E+00	-1.08202E-02	0.00000E+00
11	0.00000E+00	-1.80738E-02	0.00000E+00
12	0.00000E+00	-6.00747E-03	0.00000E+00
13	0.00000E+00	-1.18693E-02	0.00000E+00
14	0.00000E+00	-1.86642E-02	0.00000E+00
15	0.00000E+00	-1.57898E-02	0.00000E+00
16	0.00000E+00	-2.21698E-02	0.00000E+00
17	0.00000E+00	-9.66259E-03	0.00000E+00
18	0.00000E+00	-1.39212E-02	0.00000E+00
19	0.00000E+00	-1.97778E-02	0.00000E+00
20	0.00000E+00	-2.30335E-02	0.00000E+00
21	0.00000E+00	-1.92787E-02	0.00000E+00
22	0.00000E+00	-2.50375E-02	0.00000E+00
23	0.00000E+00	-3.25484E-02	0.00000E+00
24	0.00000E+00	-4.54906E-02	0.00000E+00
25	-1.03472E-02	-1.39910E-02	1.96333E-00
28	0.00000E+00	2.25310E-04	0.00000E+00
29	0.00000E+00	6.20322E-04	0.00000E+00
30	0.00000E+00	1.28842E-03	0.00000E+00
31	0.00000E+00	2.02535E-03	0.00000E+00
32	0.00000E+00	6.35896E-03	0.00000E+00
33	0.00000E+00	7.62041E-03	0.00000E+00
34	0.00000E+00	2.36728E-03	0.00000E+00
35	0.00000E+00	3.87235E-03	0.00000E+00
36	0.00000E+00	5.98956E-03	0.00000E+00
37	0.00000E+00	9.23070E-03	0.00000E+00
38	0.00000E+00	1.17843E-02	0.00000E+00
39	0.00000E+00	4.91606E-03	0.00000E+00
40	0.00000E+00	7.08906E-03	0.00000E+00
41	0.00000E+00	8.55156E-03	0.00000E+00
42	0.00000E+00	1.21162E-02	0.00000E+00
43	0.00000E+00	1.75803E-02	0.00000E+00
44	0.00000E+00	7.90558E-03	0.00000E+00
45	0.00000E+00	1.12874E-02	0.00000E+00
46	0.00000E+00	1.43904E-02	0.00000E+00
47	0.00000E+00	1.77900E-02	0.00000E+00
48	0.00000E+00	1.48160E-02	0.00000E+00
49	0.00000E+00	2.04390E-02	0.00000E+00
50	0.00000E+00	2.36665E-02	0.00000E+00
51	0.00000E+00	-4.61932E-03	0.00000E+00
52	-1.59934E-03	1.18273E-02	5.46340E-03

Table 7. 15.30 Hz, 16.0° AOA, Antisymmetric Mode Shape Listing

LOC	X	Y	Z
1	0.00000E+00	-1.28162E-03	0.00000E+00
2	0.00000E+00	-3.88983E-03	0.00000E+00
3	0.00000E+00	3.89685E-03	0.00000E+00
4	0.00000E+00	6.81007E-03	0.00000E+00
5	0.00000E+00	1.59657E-02	0.00000E+00
6	0.00000E+00	1.80605E-02	0.00000E+00
7	0.00000E+00	-5.24880E-02	0.00000E+00
8	0.00000E+00	-3.99771E-02	0.00000E+00
9	0.00000E+00	3.85686E-03	0.00000E+00
10	0.00000E+00	1.29349E-02	0.00000E+00
11	0.00000E+00	3.05167E-02	0.00000E+00
12	0.00000E+00	-8.93475E-02	0.00000E+00
13	0.00000E+00	-6.03270E-02	0.00000E+00
14	0.00000E+00	1.99369E-02	0.00000E+00
15	0.00000E+00	3.03911E-02	0.00000E+00
16	0.00000E+00	5.24419E-02	0.00000E+00
17	0.00000E+00	-1.19565E-01	0.00000E+00
18	0.00000E+00	-5.14816E-02	0.00000E+00
19	0.00000E+00	5.08917E-02	0.00000E+00
20	0.00000E+00	1.22621E-01	0.00000E+00
21	0.00000E+00	-1.18057E-01	0.00000E+00
22	0.00000E+00	5.87389E-04	0.00000E+00
23	0.00000E+00	1.29161E-01	0.00000E+00
24	0.00000E+00	3.11413E-01	0.00000E+00
25	-4.62251E-02	-7.68675E-02	2.44195E-02
28	0.00000E+00	6.06720E-04	0.00000E+00
29	0.00000E+00	3.60999E-03	0.00000E+00
30	0.00000E+00	2.36418E-03	0.00000E+00
31	0.00000E+00	9.82030E-03	0.00000E+00
32	0.00000E+00	4.99596E-02	0.00000E+00
33	0.00000E+00	5.15851E-02	0.00000E+00
34	0.00000E+00	4.67022E-02	0.00000E+00
35	0.00000E+00	3.71391E-02	0.00000E+00
36	0.00000E+00	7.20453E-03	0.00000E+00
37	0.00000E+00	1.61056E-02	0.00000E+00
38	0.00000E+00	4.53116E-02	0.00000E+00
39	0.00000E+00	9.94035E-02	0.00000E+00
40	0.00000E+00	6.25676E-02	0.00000E+00
41	0.00000E+00	-1.42565E-02	0.00000E+00
42	0.00000E+00	-1.56628E-02	0.00000E+00
43	0.00000E+00	1.32128E-02	0.00000E+00
44	0.00000E+00	1.29322E-01	0.00000E+00
45	0.00000E+00	6.02074E-02	0.00000E+00
46	0.00000E+00	-5.56244E-02	0.00000E+00
47	0.00000E+00	-1.35427E-01	0.00000E+00
48	0.00000E+00	1.30593E-01	0.00000E+00
49	0.00000E+00	-1.16748E-02	0.00000E+00
50	0.00000E+00	-1.61977E-01	0.00000E+00
51	0.00000E+00	-4.29867E-01	0.00000E+00
52	-1.83994E-02	6.92749E-02	2.91225E-02

Table 8. 44.21 Hz, 16.0° AOA, Symmetric Mode Shape Listing

LOC	X	Y	Z
1	0.00000E+00	-2.76093E-04	0.00000E+00
2	0.00000E+00	-1.01410E-03	0.00000E+00
3	0.00000E+00	8.66014E-03	0.00000E+00
4	0.00000E+00	-1.41568E-03	0.00000E+00
5	0.00000E+00	-4.77995E-02	0.00000E+00
6	0.00000E+00	-4.40221E-02	0.00000E+00
7	0.00000E+00	-5.09891E-02	0.00000E+00
8	0.00000E+00	-4.22054E-02	0.00000E+00
9	0.00000E+00	4.71058E-03	0.00000E+00
10	0.00000E+00	4.40213E-03	0.00000E+00
11	0.00000E+00	-2.69364E-02	0.00000E+00
12	0.00000E+00	-1.00554E-01	0.00000E+00
13	0.00000E+00	-6.39804E-02	0.00000E+00
14	0.00000E+00	2.15314E-02	0.00000E+00
15	0.00000E+00	2.44966E-02	0.00000E+00
16	0.00000E+00	2.81631E-03	0.00000E+00
17	0.00000E+00	-1.42693E-01	0.00000E+00
18	0.00000E+00	-6.95300E-02	0.00000E+00
19	0.00000E+00	5.39199E-02	0.00000E+00
20	0.00000E+00	1.47665E-01	0.00000E+00
21	0.00000E+00	-1.58810E-01	0.00000E+00
22	0.00000E+00	-1.37153E-02	0.00000E+00
23	0.00000E+00	1.35097E-01	0.00000E+00
24	0.00000E+00	2.40305E-01	0.00000E+00
25	-4.54780E-02	-1.06399E-01	2.80185E-02
28	0.00000E+00	-7.41001E-04	0.00000E+00
29	0.00000E+00	-2.01594E-03	0.00000E+00
30	0.00000E+00	6.54463E-03	0.00000E+00
31	0.00000E+00	-6.82052E-04	0.00000E+00
32	0.00000E+00	-4.16986E-02	0.00000E+00
33	0.00000E+00	-3.50670E-02	0.00000E+00
34	0.00000E+00	-5.32503E-02	0.00000E+00
35	0.00000E+00	-4.00380E-02	0.00000E+00
36	0.00000E+00	4.94121E-03	0.00000E+00
37	0.00000E+00	-1.54794E-03	0.00000E+00
38	0.00000E+00	-1.81538E-02	0.00000E+00
39	0.00000E+00	-9.99625E-02	0.00000E+00
40	0.00000E+00	-6.14334E-02	0.00000E+00
41	0.00000E+00	2.24091E-02	0.00000E+00
42	0.00000E+00	2.82831E-02	0.00000E+00
43	0.00000E+00	1.16025E-02	0.00000E+00
44	0.00000E+00	-1.39043E-01	0.00000E+00
45	0.00000E+00	-6.60368E-02	0.00000E+00
46	0.00000E+00	5.78052E-02	0.00000E+00
47	0.00000E+00	1.46764E-01	0.00000E+00
48	0.00000E+00	-1.50504E-01	0.00000E+00
49	0.00000E+00	-3.77370E-03	0.00000E+00
50	0.00000E+00	1.46169E-01	0.00000E+00
51	0.00000E+00	2.59571E-01	0.00000E+00
52	1.91312E-02	-9.66997E-02	-3.68326E-02

Table 9. 45.38 Hz, 16.0° AOA, AntiSymmetric Mode Shape Listing

LOC	X	Y	Z
1	0.00000E+00	-2.27848E-04	0.00000E+00
2	0.00000E+00	3.79345E-04	0.00000E+00
3	0.00000E+00	8.88690E-03	0.00000E+00
4	0.00000E+00	-3.19266E-03	0.00000E+00
5	0.00000E+00	-6.26960E-02	0.00000E+00
6	0.00000E+00	-3.56427E-02	0.00000E+00
7	0.00000E+00	-1.12760E-03	0.00000E+00
8	0.00000E+00	9.28600E-03	0.00000E+00
9	0.00000E+00	3.41842E-02	0.00000E+00
10	0.00000E+00	2.90244E-02	0.00000E+00
11	0.00000E+00	-5.55135E-03	0.00000E+00
12	0.00000E+00	-2.87066E-03	0.00000E+00
13	0.00000E+00	9.87268E-03	0.00000E+00
14	0.00000E+00	3.78960E-02	0.00000E+00
15	0.00000E+00	3.66857E-02	0.00000E+00
16	0.00000E+00	1.65184E-02	0.00000E+00
17	0.00000E+00	-9.13047E-03	0.00000E+00
18	0.00000E+00	-6.41140E-04	0.00000E+00
19	0.00000E+00	2.00233E-02	0.00000E+00
20	0.00000E+00	3.13209E-02	0.00000E+00
21	0.00000E+00	-4.66234E-02	0.00000E+00
22	0.00000E+00	-4.80444E-02	0.00000E+00
23	0.00000E+00	-5.53874E-02	0.00000E+00
24	0.00000E+00	-6.55374E-02	0.00000E+00
25	-1.38134E-02	-2.38484E-02	6.05550E-03
28	0.00000E+00	2.29294E-05	0.00000E+00
29	0.00000E+00	-1.43121E-03	0.00000E+00
30	0.00000E+00	-1.15443E-02	0.00000E+00
31	0.00000E+00	2.28874E-03	0.00000E+00
32	0.00000E+00	7.81071E-02	0.00000E+00
33	0.00000E+00	4.59974E-02	0.00000E+00
34	0.00000E+00	7.03578E-04	0.00000E+00
35	0.00000E+00	-1.14627E-02	0.00000E+00
36	0.00000E+00	-4.04296E-02	0.00000E+00
37	0.00000E+00	-3.54985E-02	0.00000E+00
38	0.00000E+00	9.35340E-03	0.00000E+00
39	0.00000E+00	3.61804E-03	0.00000E+00
40	0.00000E+00	-1.15623E-02	0.00000E+00
41	0.00000E+00	-4.61589E-02	0.00000E+00
42	0.00000E+00	-4.41871E-02	0.00000E+00
43	0.00000E+00	-1.49306E-02	0.00000E+00
44	0.00000E+00	1.20114E-02	0.00000E+00
45	0.00000E+00	1.66826E-03	0.00000E+00
46	0.00000E+00	-2.26433E-02	0.00000E+00
47	0.00000E+00	-3.55804E-02	0.00000E+00
48	0.00000E+00	5.89452E-02	0.00000E+00
49	0.00000E+00	5.78570E-02	0.00000E+00
50	0.00000E+00	6.71539E-02	0.00000E+00
51	0.00000E+00	1.31469E-02	0.00000E+00
52	-1.00093E-02	2.88018E-02	1.74842E-02

Table 10. 61.32 Hz, 16.0° AOA, Symmetric Mode Shape Listing

LOC	X	Y	Z
1	0.00000E+00	-3.37545E-04	0.00000E+00
2	0.00000E+00	-2.11103E-04	0.00000E+00
3	0.00000E+00	2.62146E-03	0.00000E+00
4	0.00000E+00	-3.77218E-03	0.00000E+00
5	0.00000E+00	-3.19503E-02	0.00000E+00
6	0.00000E+00	-1.96166E-02	0.00000E+00
7	0.00000E+00	-1.34652E-03	0.00000E+00
8	0.00000E+00	2.32194E-03	0.00000E+00
9	0.00000E+00	1.32727E-02	0.00000E+00
10	0.00000E+00	1.06497E-02	0.00000E+00
11	0.00000E+00	-6.63897E-03	0.00000E+00
12	0.00000E+00	-1.65211E-03	0.00000E+00
13	0.00000E+00	3.21007E-03	0.00000E+00
14	0.00000E+00	1.14876E-02	0.00000E+00
15	0.00000E+00	1.11872E-02	0.00000E+00
16	0.00000E+00	3.28050E-03	0.00000E+00
17	0.00000E+00	-1.90280E-03	0.00000E+00
18	0.00000E+00	1.48890E-03	0.00000E+00
19	0.00000E+00	6.68189E-03	0.00000E+00
20	0.00000E+00	9.31634E-03	0.00000E+00
21	0.00000E+00	-8.02250E-03	0.00000E+00
22	0.00000E+00	-1.25807E-02	0.00000E+00
23	0.00000E+00	-1.89107E-02	0.00000E+00
24	0.00000E+00	-1.96887E-02	0.00000E+00
25	-3.96458E-03	-5.37047E-03	2.03946E-03
28	0.00000E+00	-3.50089E-04	0.00000E+00
29	0.00000E+00	-4.26728E-05	0.00000E+00
30	0.00000E+00	2.10208E-03	0.00000E+00
31	0.00000E+00	-1.24385E-03	0.00000E+00
32	0.00000E+00	-1.92388E-02	0.00000E+00
33	0.00000E+00	-1.04093E-02	0.00000E+00
34	0.00000E+00	-1.10633E-03	0.00000E+00
35	0.00000E+00	2.07350E-03	0.00000E+00
36	0.00000E+00	9.12552E-03	0.00000E+00
37	0.00000E+00	1.06759E-02	0.00000E+00
38	0.00000E+00	1.73344E-04	0.00000E+00
39	0.00000E+00	-1.73498E-03	0.00000E+00
40	0.00000E+00	2.83300E-03	0.00000E+00
41	0.00000E+00	1.18526E-02	0.00000E+00
42	0.00000E+00	1.22357E-02	0.00000E+00
43	0.00000E+00	8.68614E-03	0.00000E+00
44	0.00000E+00	-2.71575E-03	0.00000E+00
45	0.00000E+00	4.26070E-04	0.00000E+00
46	0.00000E+00	5.42131E-03	0.00000E+00
47	0.00000E+00	7.96747E-03	0.00000E+00
48	0.00000E+00	-1.13833E-02	0.00000E+00
49	0.00000E+00	-1.37872E-02	0.00000E+00
50	0.00000E+00	-1.96258E-02	0.00000E+00
51	0.00000E+00	1.59241E-02	0.00000E+00
52	-8.80503E-04	-4.51115E-03	-2.37491E-03

Table 11. 61.94 Hz, 16.0° AOA, Antisymmetric Mode Shape Listing

LOC	X	Y	Z
1	0.00000E+00	5.94502E-04	0.00000E+00
2	0.00000E+00	-1.12238E-03	0.00000E+00
3	0.00000E+00	-4.56818E-03	0.00000E+00
4	0.00000E+00	-8.61252E-03	0.00000E+00
5	0.00000E+00	-2.18819E-02	0.00000E+00
6	0.00000E+00	-3.69463E-02	0.00000E+00
7	0.00000E+00	-9.49052E-03	0.00000E+00
8	0.00000E+00	-1.88902E-02	0.00000E+00
9	0.00000E+00	-3.62481E-02	0.00000E+00
10	0.00000E+00	-4.01400E-02	0.00000E+00
11	0.00000E+00	-5.55564E-02	0.00000E+00
12	0.00000E+00	-2.13678E-02	0.00000E+00
13	0.00000E+00	-3.58586E-02	0.00000E+00
14	0.00000E+00	-5.09872E-02	0.00000E+00
15	0.00000E+00	-5.28957E-02	0.00000E+00
16	0.00000E+00	-6.57138E-02	0.00000E+00
17	0.00000E+00	-3.55358E-02	0.00000E+00
18	0.00000E+00	-5.19799E-02	0.00000E+00
19	0.00000E+00	-6.92835E-02	0.00000E+00
20	0.00000E+00	-8.37365E-02	0.00000E+00
21	0.00000E+00	-7.37355E-02	0.00000E+00
22	0.00000E+00	-9.28192E-02	0.00000E+00
23	0.00000E+00	-1.13240E-01	0.00000E+00
24	0.00000E+00	-1.45870E-01	0.00000E+00
25	-3.90873E-02	-6.80519E-02	1.25732E-02
28	0.00000E+00	3.24246E-04	0.00000E+00
29	0.00000E+00	-9.18207E-04	0.00000E+00
30	0.00000E+00	-2.71056E-03	0.00000E+00
31	0.00000E+00	-4.31144E-03	0.00000E+00
32	0.00000E+00	-1.18242E-02	0.00000E+00
33	0.00000E+00	-1.83085E-02	0.00000E+00
34	0.00000E+00	-6.55448E-03	0.00000E+00
35	0.00000E+00	-1.17379E-02	0.00000E+00
36	0.00000E+00	-1.74948E-02	0.00000E+00
37	0.00000E+00	-3.04250E-02	0.00000E+00
38	0.00000E+00	-3.38806E-02	0.00000E+00
39	0.00000E+00	-1.64052E-02	0.00000E+00
40	0.00000E+00	-2.61968E-02	0.00000E+00
41	0.00000E+00	-3.49554E-02	0.00000E+00
42	0.00000E+00	-3.98500E-02	0.00000E+00
43	0.00000E+00	-5.12396E-02	0.00000E+00
44	0.00000E+00	-2.65726E-02	0.00000E+00
45	0.00000E+00	-3.93173E-02	0.00000E+00
46	0.00000E+00	-4.94785E-02	0.00000E+00
47	0.00000E+00	-6.19442E-02	0.00000E+00
48	0.00000E+00	-5.33055E-02	0.00000E+00
49	0.00000E+00	-6.62531E-02	0.00000E+00
50	0.00000E+00	-8.15127E-02	0.00000E+00
51	0.00000E+00	-8.29448E-02	0.00000E+00
52	3.96340E-03	-3.42748E-02	-1.50788E-02

Table 12. 15.13 Hz, 28.8° AOA, Anisymmetric Mode Shape Listing

LOC	X	Y	Z
1	0.00000E+00	9.31684E-05	0.00000E+00
2	0.00000E+00	-1.44130E-04	0.00000E+00
3	0.00000E+00	-9.94606E-04	0.00000E+00
4	0.00000E+00	-1.91798E-03	0.00000E+00
5	0.00000E+00	-4.91379E-03	0.00000E+00
6	0.00000E+00	-8.20088E-03	0.00000E+00
7	0.00000E+00	-2.57482E-03	0.00000E+00
8	0.00000E+00	-5.57279E-03	0.00000E+00
9	0.00000E+00	-7.91084E-03	0.00000E+00
10	0.00000E+00	-8.78625E-03	0.00000E+00
11	0.00000E+00	-1.23229E-02	0.00000E+00
12	0.00000E+00	-6.09627E-03	0.00000E+00
13	0.00000E+00	-1.05967E-02	0.00000E+00
14	0.00000E+00	-1.58120E-02	0.00000E+00
15	0.00000E+00	-1.62566E-02	0.00000E+00
16	0.00000E+00	-2.05468E-02	0.00000E+00
17	0.00000E+00	-1.05075E-02	0.00000E+00
18	0.00000E+00	-1.58405E-02	0.00000E+00
19	0.00000E+00	-2.12698E-02	0.00000E+00
20	0.00000E+00	-2.57800E-02	0.00000E+00
21	0.00000E+00	-2.26812E-02	0.00000E+00
22	0.00000E+00	-2.85040E-02	0.00000E+00
23	0.00000E+00	-3.46806E-02	0.00000E+00
24	0.00000E+00	-4.46511E-02	0.00000E+00
25	-7.93418E-03	-1.51853E-02	2.62564E-03
28	0.00000E+00	-4.24745E-04	0.00000E+00
29	0.00000E+00	7.20067E-04	0.00000E+00
30	0.00000E+00	2.84544E-03	0.00000E+00
31	0.00000E+00	4.65782E-03	0.00000E+00
32	0.00000E+00	1.34265E-02	0.00000E+00
33	0.00000E+00	2.07419E-02	0.00000E+00
34	0.00000E+00	6.83819E-03	0.00000E+00
35	0.00000E+00	1.29048E-02	0.00000E+00
36	0.00000E+00	1.96563E-02	0.00000E+00
37	0.00000E+00	3.06528E-02	0.00000E+00
38	0.00000E+00	3.34527E-02	0.00000E+00
39	0.00000E+00	1.56050E-02	0.00000E+00
40	0.00000E+00	2.55197E-02	0.00000E+00
41	0.00000E+00	3.42430E-02	0.00000E+00
42	0.00000E+00	3.92044E-02	0.00000E+00
43	0.00000E+00	5.16933E-02	0.00000E+00
44	0.00000E+00	2.55981E-02	0.00000E+00
45	0.00000E+00	3.84217E-02	0.00000E+00
46	0.00000E+00	4.85564E-02	0.00000E+00
47	0.00000E+00	6.11195E-02	0.00000E+00
48	0.00000E+00	5.23864E-02	0.00000E+00
49	0.00000E+00	6.52587E-02	0.00000E+00
50	0.00000E+00	8.06005E-02	0.00000E+00
51	0.00000E+00	8.20384E-02	0.00000E+00
52	-2.43329E-03	3.96901E-02	1.55660E-02

Table 13. 15.44 Hz, 28.8° AOA, Symmetric Mode Shape Listing

LOC	X	Y	Z
1	0.00000E+00	-1.17967E-03	0.00000E+00
2	0.00000E+00	-5.09213E-03	0.00000E+00
3	0.00000E+00	4.38309E-03	0.00000E+00
4	0.00000E+00	-1.52149E-03	0.00000E+00
5	0.00000E+00	-3.00980E-02	0.00000E+00
6	0.00000E+00	-2.81339E-02	0.00000E+00
7	0.00000E+00	-6.96438E-02	0.00000E+00
8	0.00000E+00	-5.60874E-02	0.00000E+00
9	0.00000E+00	3.18922E-03	0.00000E+00
10	0.00000E+00	7.83280E-03	0.00000E+00
11	0.00000E+00	-6.61026E-03	0.00000E+00
12	0.00000E+00	-1.27271E-01	0.00000E+00
13	0.00000E+00	-7.98845E-02	0.00000E+00
14	0.00000E+00	2.70301E-02	0.00000E+00
15	0.00000E+00	3.54765E-02	0.00000E+00
16	0.00000E+00	2.80791E-02	0.00000E+00
17	0.00000E+00	-1.74376E-01	0.00000E+00
18	0.00000E+00	-7.84824E-02	0.00000E+00
19	0.00000E+00	7.35194E-02	0.00000E+00
20	0.00000E+00	1.85500E-01	0.00000E+00
21	0.00000E+00	-1.78256E-01	0.00000E+00
22	0.00000E+00	-1.31609E-03	0.00000E+00
23	0.00000E+00	1.86209E-01	0.00000E+00
24	0.00000E+00	3.80316E-01	0.00000E+00
25	-6.23576E-02	-1.16290E-01	4.51923E-02
28	0.00000E+00	1.52961E-03	0.00000E+00
29	0.00000E+00	4.86126E-03	0.00000E+00
30	0.00000E+00	-2.78631E-03	0.00000E+00
31	0.00000E+00	2.96398E-04	0.00000E+00
32	0.00000E+00	2.14562E-02	0.00000E+00
33	0.00000E+00	1.45542E-02	0.00000E+00
34	0.00000E+00	6.28159E-02	0.00000E+00
35	0.00000E+00	4.72274E-02	0.00000E+00
36	0.00000E+00	-1.96568E-03	0.00000E+00
37	0.00000E+00	-4.38989E-03	0.00000E+00
38	0.00000E+00	-4.61070E-03	0.00000E+00
39	0.00000E+00	1.06812E-01	0.00000E+00
40	0.00000E+00	6.35561E-02	0.00000E+00
41	0.00000E+00	-2.14349E-02	0.00000E+00
42	0.00000E+00	-3.24220E-02	0.00000E+00
43	0.00000E+00	-3.79236E-02	0.00000E+00
44	0.00000E+00	1.40424E-01	0.00000E+00
45	0.00000E+00	6.28716E-02	0.00000E+00
46	0.00000E+00	-6.19168E-02	0.00000E+00
47	0.00000E+00	-1.49547E-01	0.00000E+00
48	0.00000E+00	1.33485E-01	0.00000E+00
49	0.00000E+00	-8.70723E-03	0.00000E+00
50	0.00000E+00	-1.54016E-01	0.00000E+00
51	0.00000E+00	-2.38111E-01	0.00000E+00
52	-2.31971E-02	9.14430E-02	3.76912E-02

Table 14. 43.95 Hz, 28.8° AOA, Symmetric Mode Shape Listing

LOC	X	Y	Z
1	0.00000E+00	1.05664E-04	0.00000E+00
2	0.00000E+00	-6.51856E-04	0.00000E+00
3	0.00000E+00	8.32681E-03	0.00000E+00
4	0.00000E+00	-1.40873E-03	0.00000E+00
5	0.00000E+00	-4.56916E-02	0.00000E+00
6	0.00000E+00	-4.44775E-02	0.00000E+00
7	0.00000E+00	-4.75159E-02	0.00000E+00
8	0.00000E+00	-3.81769E-02	0.00000E+00
9	0.00000E+00	6.73556E-03	0.00000E+00
10	0.00000E+00	5.73380E-03	0.00000E+00
11	0.00000E+00	-2.80146E-02	0.00000E+00
12	0.00000E+00	-9.26815E-02	0.00000E+00
13	0.00000E+00	-5.78561E-02	0.00000E+00
14	0.00000E+00	2.10996E-02	0.00000E+00
15	0.00000E+00	2.44413E-02	0.00000E+00
16	0.00000E+00	-2.54827E-03	0.00000E+00
17	0.00000E+00	-1.32431E-01	0.00000E+00
18	0.00000E+00	-6.27412E-02	0.00000E+00
19	0.00000E+00	5.30704E-02	0.00000E+00
20	0.00000E+00	1.40098E-01	0.00000E+00
21	0.00000E+00	-1.47824E-01	0.00000E+00
22	0.00000E+00	-1.35787E-02	0.00000E+00
23	0.00000E+00	1.28046E-01	0.00000E+00
24	0.00000E+00	2.62621E-01	0.00000E+00
25	-4.55868E-02	-9.99615E-02	2.89231E-02
28	0.00000E+00	-3.88968E-04	0.00000E+00
29	0.00000E+00	-1.57455E-03	0.00000E+00
30	0.00000E+00	8.66080E-03	0.00000E+00
31	0.00000E+00	7.69000E-04	0.00000E+00
32	0.00000E+00	-4.52800E-02	0.00000E+00
33	0.00000E+00	-3.56697E-02	0.00000E+00
34	0.00000E+00	-5.79953E-02	0.00000E+00
35	0.00000E+00	-4.26391E-02	0.00000E+00
36	0.00000E+00	8.40787E-03	0.00000E+00
37	0.00000E+00	7.47956E-03	0.00000E+00
38	0.00000E+00	-1.50380E-02	0.00000E+00
39	0.00000E+00	-1.08884E-01	0.00000E+00
40	0.00000E+00	-6.54545E-02	0.00000E+00
41	0.00000E+00	2.60325E-02	0.00000E+00
42	0.00000E+00	3.24874E-02	0.00000E+00
43	0.00000E+00	1.77305E-02	0.00000E+00
44	0.00000E+00	-1.48152E-01	0.00000E+00
45	0.00000E+00	-6.99454E-02	0.00000E+00
46	0.00000E+00	6.06977E-02	0.00000E+00
47	0.00000E+00	1.54556E-01	0.00000E+00
48	0.00000E+00	-1.58675E-01	0.00000E+00
49	0.00000E+00	-8.28317E-03	0.00000E+00
50	0.00000E+00	1.46313E-01	0.00000E+00
51	0.00000E+00	2.39910E-01	0.00000E+00
52	1.78948E-02	-1.05965E-01	-3.88652E-02

Table 15. 45.12 Hz, 28.8° AOA, Antisymmetric Mode Shape Listing

LOC	X	Y	Z
1	0.00000E+00	-3.05320E-04	0.00000E+00
2	0.00000E+00	1.73962E-03	0.00000E+00
3	0.00000E+00	1.78818E-02	0.00000E+00
4	0.00000E+00	-6.67140E-03	0.00000E+00
5	0.00000E+00	-1.23319E-01	0.00000E+00
6	0.00000E+00	-7.83145E-02	0.00000E+00
7	0.00000E+00	-2.06875E-04	0.00000E+00
8	0.00000E+00	1.96757E-02	0.00000E+00
9	0.00000E+00	6.72109E-02	0.00000E+00
10	0.00000E+00	5.43728E-02	0.00000E+00
11	0.00000E+00	-2.32221E-02	0.00000E+00
12	0.00000E+00	-2.60138E-03	0.00000E+00
13	0.00000E+00	2.09594E-02	0.00000E+00
14	0.00000E+00	7.08723E-02	0.00000E+00
15	0.00000E+00	6.73047E-02	0.00000E+00
16	0.00000E+00	1.16025E-02	0.00000E+00
17	0.00000E+00	-1.40777E-02	0.00000E+00
18	0.00000E+00	4.00987E-04	0.00000E+00
19	0.00000E+00	3.84774E-02	0.00000E+00
20	0.00000E+00	5.83664E-02	0.00000E+00
21	0.00000E+00	-8.75640E-02	0.00000E+00
22	0.00000E+00	-9.21293E-02	0.00000E+00
23	0.00000E+00	-1.11800E-01	0.00000E+00
24	0.00000E+00	-1.55740E-01	0.00000E+00
25	-2.71150E-02	-4.46668E-02	1.27504E-02
28	0.00000E+00	8.36694E-04	0.00000E+00
29	0.00000E+00	-6.70050E-04	0.00000E+00
30	0.00000E+00	-1.12737E-02	0.00000E+00
31	0.00000E+00	3.79606E-03	0.00000E+00
32	0.00000E+00	8.82271E-02	0.00000E+00
33	0.00000E+00	4.80609E-02	0.00000E+00
34	0.00000E+00	1.16875E-03	0.00000E+00
35	0.00000E+00	-1.25108E-02	0.00000E+00
36	0.00000E+00	-4.52756E-02	0.00000E+00
37	0.00000E+00	-3.95568E-02	0.00000E+00
38	0.00000E+00	4.48358E-03	0.00000E+00
39	0.00000E+00	2.97606E-03	0.00000E+00
40	0.00000E+00	-1.27466E-02	0.00000E+00
41	0.00000E+00	-4.80755E-02	0.00000E+00
42	0.00000E+00	-4.62220E-02	0.00000E+00
43	0.00000E+00	-2.28095E-02	0.00000E+00
44	0.00000E+00	9.82300E-03	0.00000E+00
45	0.00000E+00	6.36173E-05	0.00000E+00
46	0.00000E+00	-2.29751E-02	0.00000E+00
47	0.00000E+00	-3.47031E-02	0.00000E+00
48	0.00000E+00	5.63666E-02	0.00000E+00
49	0.00000E+00	6.07041E-02	0.00000E+00
50	0.00000E+00	7.58362E-02	0.00000E+00
51	0.00000E+00	8.87214E-02	0.00000E+00
52	-2.22742E-03	3.14741E-02	1.61248E-02

Table 16. 61.55 Hz, 28.8° AOA, Symmetric Mode Shape Listing

LOC	X	Y	Z
1	0.00000E+00	-1.98708E-04	0.00000E+00
2	0.00000E+00	4.79090E-04	0.00000E+00
3	0.00000E+00	4.10324E-03	0.00000E+00
4	0.00000E+00	-1.34828E-03	0.00000E+00
5	0.00000E+00	-2.69189E-02	0.00000E+00
6	0.00000E+00	-1.75761E-02	0.00000E+00
7	0.00000E+00	-5.87386E-04	0.00000E+00
8	0.00000E+00	3.90508E-03	0.00000E+00
9	0.00000E+00	1.42599E-02	0.00000E+00
10	0.00000E+00	1.13465E-02	0.00000E+00
11	0.00000E+00	-5.89358E-03	0.00000E+00
12	0.00000E+00	-9.58618E-04	0.00000E+00
13	0.00000E+00	4.41271E-03	0.00000E+00
14	0.00000E+00	1.47134E-02	0.00000E+00
15	0.00000E+00	1.36842E-02	0.00000E+00
16	0.00000E+00	1.73329E-03	0.00000E+00
17	0.00000E+00	-2.63885E-03	0.00000E+00
18	0.00000E+00	5.93808E-04	0.00000E+00
19	0.00000E+00	7.88404E-03	0.00000E+00
20	0.00000E+00	1.15400E-02	0.00000E+00
21	0.00000E+00	-1.57366E-02	0.00000E+00
22	0.00000E+00	-1.79408E-02	0.00000E+00
23	0.00000E+00	-2.35694E-02	0.00000E+00
24	0.00000E+00	-3.42816E-02	0.00000E+00
25	-5.23461E-03	-7.89813E-03	1.69516E-03
28	0.00000E+00	-5.10837E-04	0.00000E+00
29	0.00000E+00	9.87555E-04	0.00000E+00
30	0.00000E+00	8.53501E-03	0.00000E+00
31	0.00000E+00	-2.81887E-03	0.00000E+00
32	0.00000E+00	-6.62524E-02	0.00000E+00
33	0.00000E+00	-3.83877E-02	0.00000E+00
34	0.00000E+00	-1.34070E-03	0.00000E+00
35	0.00000E+00	9.01068E-03	0.00000E+00
36	0.00000E+00	3.28229E-02	0.00000E+00
37	0.00000E+00	2.82019E-02	0.00000E+00
38	0.00000E+00	-6.82302E-03	0.00000E+00
39	0.00000E+00	-3.02897E-03	0.00000E+00
40	0.00000E+00	9.17477E-03	0.00000E+00
41	0.00000E+00	3.51523E-02	0.00000E+00
42	0.00000E+00	3.27471E-02	0.00000E+00
43	0.00000E+00	1.44301E-02	0.00000E+00
44	0.00000E+00	-7.18464E-03	0.00000E+00
45	0.00000E+00	6.31921E-04	0.00000E+00
46	0.00000E+00	1.70651E-02	0.00000E+00
47	0.00000E+00	2.49106E-02	0.00000E+00
48	0.00000E+00	-3.77747E-02	0.00000E+00
49	0.00000E+00	-4.24911E-02	0.00000E+00
50	0.00000E+00	-5.49665E-02	0.00000E+00
51	0.00000E+00	-6.59712E-02	0.00000E+00
52	6.70285E-04	-2.10916E-02	-1.09855E-02

Table 17. 62.19 Hz, 28.8° AOA, Antisymmetric Mode Shape Listing

LOC	X	Y	Z
1	0.00000E+00	1.07471E-03	0.00000E+00
2	0.00000E+00	-1.09504E-03	0.00000E+00
3	0.00000E+00	-5.62489E-03	0.00000E+00
4	0.00000E+00	-1.10209E-02	0.00000E+00
5	0.00000E+00	-3.11287E-02	0.00000E+00
6	0.00000E+00	-4.89944E-02	0.00000E+00
7	0.00000E+00	-1.35064E-02	0.00000E+00
8	0.00000E+00	-2.73042E-02	0.00000E+00
9	0.00000E+00	-4.55542E-02	0.00000E+00
10	0.00000E+00	-5.12866E-02	0.00000E+00
11	0.00000E+00	-7.26075E-02	0.00000E+00
12	0.00000E+00	-3.04744E-02	0.00000E+00
13	0.00000E+00	-5.13837E-02	0.00000E+00
14	0.00000E+00	-7.57565E-02	0.00000E+00
15	0.00000E+00	-7.65823E-02	0.00000E+00
16	0.00000E+00	-9.53600E-02	0.00000E+00
17	0.00000E+00	-5.13558E-02	0.00000E+00
18	0.00000E+00	-7.48142E-02	0.00000E+00
19	0.00000E+00	-1.00509E-01	0.00000E+00
20	0.00000E+00	-1.20141E-01	0.00000E+00
21	0.00000E+00	-1.06080E-01	0.00000E+00
22	0.00000E+00	-1.88729E-01	0.00000E+00
23	0.00000E+00	-1.62666E-01	0.00000E+00
24	0.00000E+00	-2.00616E-01	0.00000E+00
25	-4.84908E-02	-8.47875E-02	1.57851E-02
28	0.00000E+00	4.39754E-04	0.00000E+00
29	0.00000E+00	-9.89014E-04	0.00000E+00
30	0.00000E+00	-2.91016E-03	0.00000E+00
31	0.00000E+00	-6.62627E-03	0.00000E+00
32	0.00000E+00	-2.51982E-02	0.00000E+00
33	0.00000E+00	-2.98744E-02	0.00000E+00
34	0.00000E+00	-6.67586E-03	0.00000E+00
35	0.00000E+00	-1.17938E-02	0.00000E+00
36	0.00000E+00	-1.76220E-02	0.00000E+00
37	0.00000E+00	-2.40900E-02	0.00000E+00
38	0.00000E+00	-3.24717E-02	0.00000E+00
39	0.00000E+00	-1.30505E-02	0.00000E+00
40	0.00000E+00	-2.05335E-02	0.00000E+00
41	0.00000E+00	-2.73141E-02	0.00000E+00
42	0.00000E+00	-3.28485E-02	0.00000E+00
43	0.00000E+00	-4.44401E-02	0.00000E+00
44	0.00000E+00	-2.12877E-02	0.00000E+00
45	0.00000E+00	-3.09952E-02	0.00000E+00
46	0.00000E+00	-3.87810E-02	0.00000E+00
47	0.00000E+00	-4.89455E-02	0.00000E+00
48	0.00000E+00	-4.15552E-02	0.00000E+00
49	0.00000E+00	-5.18115E-02	0.00000E+00
50	0.00000E+00	-6.39570E-02	0.00000E+00
51	0.00000E+00	-6.68235E-02	0.00000E+00
52	4.43120E-03	-3.39942E-02	-1.55824E-02

Table 18. 15.11 Hz, 45.5° AOA, Antisymmetric Mode Shape Listing

LOC	X	Y	Z
1	0.00000E+00	5.60001E-04	0.00000E+00
2	0.00000E+00	7.16969E-04	0.00000E+00
3	0.00000E+00	1.68120E-04	0.00000E+00
4	0.00000E+00	-3.58576E-06	0.00000E+00
5	0.00000E+00	2.24828E-04	0.00000E+00
6	0.00000E+00	-1.78296E-03	0.00000E+00
7	0.00000E+00	-1.04172E-03	0.00000E+00
8	0.00000E+00	-2.96451E-03	0.00000E+00
9	0.00000E+00	-4.06010E-03	0.00000E+00
10	0.00000E+00	-4.15702E-03	0.00000E+00
11	0.00000E+00	-4.63133E-03	0.00000E+00
12	0.00000E+00	-3.24648E-03	0.00000E+00
13	0.00000E+00	-4.80230E-03	0.00000E+00
14	0.00000E+00	-7.02725E-03	0.00000E+00
15	0.00000E+00	-8.91614E-03	0.00000E+00
16	0.00000E+00	-9.99282E-03	0.00000E+00
17	0.00000E+00	-5.99179E-03	0.00000E+00
18	0.00000E+00	-9.49653E-03	0.00000E+00
19	0.00000E+00	-1.24900E-02	0.00000E+00
20	0.00000E+00	-1.55488E-02	0.00000E+00
21	0.00000E+00	-1.32029E-02	0.00000E+00
22	0.00000E+00	-2.44021E-02	0.00000E+00
23	0.00000E+00	-2.01513E-02	0.00000E+00
24	0.00000E+00	-2.08779E-02	0.00000E+00
25	-1.90070E-03	-9.76367E-03	-6.20019E-04
28	0.00000E+00	-7.26055E-04	0.00000E+00
29	0.00000E+00	-5.41702E-04	0.00000E+00
30	0.00000E+00	2.01884E-04	0.00000E+00
31	0.00000E+00	-1.44420E-03	0.00000E+00
32	0.00000E+00	-1.18466E-02	0.00000E+00
33	0.00000E+00	-4.85285E-03	0.00000E+00
34	0.00000E+00	2.59668E-03	0.00000E+00
35	0.00000E+00	5.69442E-03	0.00000E+00
36	0.00000E+00	8.42405E-03	0.00000E+00
37	0.00000E+00	1.18999E-02	0.00000E+00
38	0.00000E+00	3.61443E-03	0.00000E+00
39	0.00000E+00	7.10340E-03	0.00000E+00
40	0.00000E+00	1.25906E-02	0.00000E+00
41	0.00000E+00	1.78181E-02	0.00000E+00
42	0.00000E+00	1.70167E-02	0.00000E+00
43	0.00000E+00	1.37805E-02	0.00000E+00
44	0.00000E+00	1.21434E-02	0.00000E+00
45	0.00000E+00	1.85677E-02	0.00000E+00
46	0.00000E+00	2.33746E-02	0.00000E+00
47	0.00000E+00	3.01530E-02	0.00000E+00
48	0.00000E+00	2.61165E-02	0.00000E+00
49	0.00000E+00	3.04924E-02	0.00000E+00
50	0.00000E+00	4.00685E-02	0.00000E+00
51	0.00000E+00	4.39005E-02	0.00000E+00
52	5.23592E-04	1.91453E-02	5.18429E-03

Table 19. 15.64 Hz, 45.5° AOA, Symmetric Mode Shape Listing

LOC	X	Y	Z
1	0.00000E+00	-4.53269E-04	0.00000E+00
2	0.00000E+00	-2.53876E-03	0.00000E+00
3	0.00000E+00	3.69158E-03	0.00000E+00
4	0.00000E+00	2.58926E-03	0.00000E+00
5	0.00000E+00	-4.74994E-03	0.00000E+00
6	0.00000E+00	3.24626E-04	0.00000E+00
7	0.00000E+00	-3.22622E-02	0.00000E+00
8	0.00000E+00	-2.36651E-02	0.00000E+00
9	0.00000E+00	6.11132E-03	0.00000E+00
10	0.00000E+00	1.04312E-02	0.00000E+00
11	0.00000E+00	1.34515E-02	0.00000E+00
12	0.00000E+00	-5.65271E-02	0.00000E+00
13	0.00000E+00	-3.40295E-02	0.00000E+00
14	0.00000E+00	1.65456E-02	0.00000E+00
15	0.00000E+00	2.26780E-02	0.00000E+00
16	0.00000E+00	3.09723E-02	0.00000E+00
17	0.00000E+00	-7.61167E-02	0.00000E+00
18	0.00000E+00	-3.15970E-02	0.00000E+00
19	0.00000E+00	3.43103E-02	0.00000E+00
20	0.00000E+00	7.94148E-02	0.00000E+00
21	0.00000E+00	-7.38385E-02	0.00000E+00
22	0.00000E+00	-3.70969E-03	0.00000E+00
23	0.00000E+00	7.44437E-02	0.00000E+00
24	0.00000E+00	1.62038E-01	0.00000E+00
25	-3.05939E-02	-4.63004E-02	2.39675E-02
28	0.00000E+00	7.95641E-04	0.00000E+00
29	0.00000E+00	2.84744E-03	0.00000E+00
30	0.00000E+00	-1.27419E-03	0.00000E+00
31	0.00000E+00	-7.11976E-04	0.00000E+00
32	0.00000E+00	5.39360E-03	0.00000E+00
33	0.00000E+00	3.85068E-04	0.00000E+00
34	0.00000E+00	3.02007E-02	0.00000E+00
35	0.00000E+00	2.27321E-02	0.00000E+00
36	0.00000E+00	-2.40788E-03	0.00000E+00
37	0.00000E+00	-2.45673E-03	0.00000E+00
38	0.00000E+00	-9.84254E-03	0.00000E+00
39	0.00000E+00	5.13275E-02	0.00000E+00
40	0.00000E+00	2.98377E-02	0.00000E+00
41	0.00000E+00	-1.11951E-02	0.00000E+00
42	0.00000E+00	-1.85192E-02	0.00000E+00
43	0.00000E+00	-2.59953E-02	0.00000E+00
44	0.00000E+00	6.94089E-02	0.00000E+00
45	0.00000E+00	2.97460E-02	0.00000E+00
46	0.00000E+00	-3.14488E-02	0.00000E+00
47	0.00000E+00	-7.47006E-02	0.00000E+00
48	0.00000E+00	6.30823E-02	0.00000E+00
49	0.00000E+00	-6.13913E-03	0.00000E+00
50	0.00000E+00	-7.27241E-02	0.00000E+00
51	0.00000E+00	-1.08363E-01	0.00000E+00
52	-1.09538E-02	4.18716E-02	1.73673E-02

Table 20. 43.92 Hz, 45.5° AOA, Symmetric Mode Shape Listing

LOC	X	Y	Z
1	0.00000E+00	3.40334E-04	0.00000E+00
2	0.00000E+00	2.45810E-04	0.00000E+00
3	0.00000E+00	8.98745E-03	0.00000E+00
4	0.00000E+00	1.37575E-03	0.00000E+00
5	0.00000E+00	-3.60617E-02	0.00000E+00
6	0.00000E+00	-3.24673E-02	0.00000E+00
7	0.00000E+00	-3.41893E-02	0.00000E+00
8	0.00000E+00	-2.66755E-02	0.00000E+00
9	0.00000E+00	9.14618E-03	0.00000E+00
10	0.00000E+00	8.21175E-03	0.00000E+00
11	0.00000E+00	-1.96189E-02	0.00000E+00
12	0.00000E+00	-6.76296E-02	0.00000E+00
13	0.00000E+00	-4.10262E-02	0.00000E+00
14	0.00000E+00	1.81885E-02	0.00000E+00
15	0.00000E+00	2.06275E-02	0.00000E+00
16	0.00000E+00	-5.63806E-04	0.00000E+00
17	0.00000E+00	-9.78149E-02	0.00000E+00
18	0.00000E+00	-4.59005E-02	0.00000E+00
19	0.00000E+00	4.00456E-02	0.00000E+00
20	0.00000E+00	1.03378E-01	0.00000E+00
21	0.00000E+00	-1.10391E-01	0.00000E+00
22	0.00000E+00	-1.89552E-02	0.00000E+00
23	0.00000E+00	8.88221E-02	0.00000E+00
24	0.00000E+00	1.70173E-01	0.00000E+00
25	-3.58171E-02	-7.83960E-02	2.30681E-02
28	0.00000E+00	-1.47544E-04	0.00000E+00
29	0.00000E+00	-1.27438E-03	0.00000E+00
30	0.00000E+00	1.02409E-02	0.00000E+00
31	0.00000E+00	3.06033E-03	0.00000E+00
32	0.00000E+00	-3.92559E-02	0.00000E+00
33	0.00000E+00	-2.85078E-02	0.00000E+00
34	0.00000E+00	-6.06442E-02	0.00000E+00
35	0.00000E+00	-4.43905E-02	0.00000E+00
36	0.00000E+00	9.92513E-03	0.00000E+00
37	0.00000E+00	1.24544E-02	0.00000E+00
38	0.00000E+00	-1.83713E-03	0.00000E+00
39	0.00000E+00	-1.05760E-01	0.00000E+00
40	0.00000E+00	-6.30265E-02	0.00000E+00
41	0.00000E+00	2.60930E-02	0.00000E+00
42	0.00000E+00	3.57307E-02	0.00000E+00
43	0.00000E+00	3.15146E-02	0.00000E+00
44	0.00000E+00	-1.45121E-01	0.00000E+00
45	0.00000E+00	-6.80205E-02	0.00000E+00
46	0.00000E+00	5.81000E-02	0.00000E+00
47	0.00000E+00	1.49449E-01	0.00000E+00
48	0.00000E+00	-1.55682E-01	0.00000E+00
49	0.00000E+00	-9.46798E-03	0.00000E+00
50	0.00000E+00	1.38254E-01	0.00000E+00
51	0.00000E+00	2.34113E-01	0.00000E+00
52	1.97364E-02	-1.11047E-01	-4.10834E-02

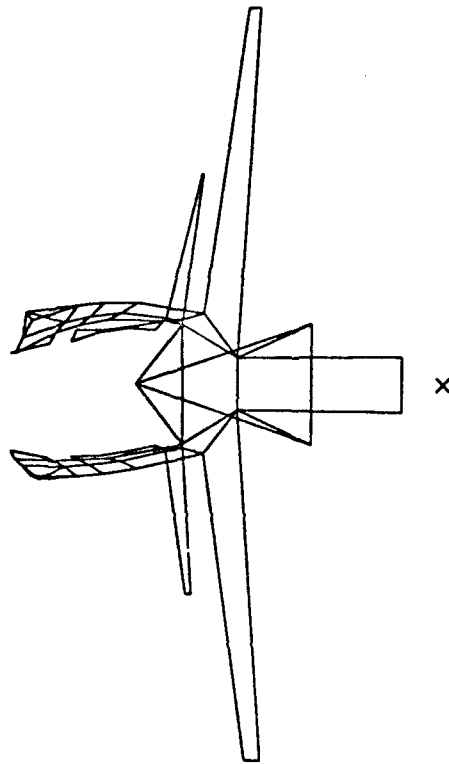
Table 21. 45.36 Hz, 45.5° AOA, Anisymmetric Mode Shape Listing

LOC	X	Y	Z
1	0.00000E+00	3.48152E-04	0.00000E+00
2	0.00000E+00	4.87806E-04	0.00000E+00
3	0.00000E+00	4.23753E-04	0.00000E+00
4	0.00000E+00	-6.18836E-04	0.00000E+00
5	0.00000E+00	-6.24724E-03	0.00000E+00
6	0.00000E+00	-6.58237E-03	0.00000E+00
7	0.00000E+00	6.81679E-04	0.00000E+00
8	0.00000E+00	2.85163E-03	0.00000E+00
9	0.00000E+00	1.81711E-03	0.00000E+00
10	0.00000E+00	3.24961E-04	0.00000E+00
11	0.00000E+00	-7.16936E-03	0.00000E+00
12	0.00000E+00	3.64376E-04	0.00000E+00
13	0.00000E+00	2.65656E-03	0.00000E+00
14	0.00000E+00	8.60275E-03	0.00000E+00
15	0.00000E+00	7.58279E-03	0.00000E+00
16	0.00000E+00	-3.61424E-03	0.00000E+00
17	0.00000E+00	-1.47217E-03	0.00000E+00
18	0.00000E+00	2.49346E-04	0.00000E+00
19	0.00000E+00	5.54754E-03	0.00000E+00
20	0.00000E+00	8.70558E-03	0.00000E+00
21	0.00000E+00	-1.19417E-02	0.00000E+00
22	0.00000E+00	-1.61616E-02	0.00000E+00
23	0.00000E+00	-1.19192E-02	0.00000E+00
24	0.00000E+00	-1.01821E-02	0.00000E+00
25	-1.09569E-03	-1.12221E-03	1.57322E-03
28	0.00000E+00	3.97526E-04	0.00000E+00
29	0.00000E+00	4.79485E-04	0.00000E+00
30	0.00000E+00	3.97572E-04	0.00000E+00
31	0.00000E+00	2.14076E-03	0.00000E+00
32	0.00000E+00	1.15704E-02	0.00000E+00
33	0.00000E+00	9.48221E-03	0.00000E+00
34	0.00000E+00	1.44575E-04	0.00000E+00
35	0.00000E+00	-1.25680E-03	0.00000E+00
36	0.00000E+00	-3.86960E-03	0.00000E+00
37	0.00000E+00	5.09266E-05	0.00000E+00
38	0.00000E+00	2.83447E-03	0.00000E+00
39	0.00000E+00	-4.14656E-04	0.00000E+00
40	0.00000E+00	-2.40802E-03	0.00000E+00
41	0.00000E+00	-8.31592E-03	0.00000E+00
42	0.00000E+00	-6.80496E-03	0.00000E+00
43	0.00000E+00	-1.19147E-03	0.00000E+00
44	0.00000E+00	-4.31974E-04	0.00000E+00
45	0.00000E+00	-1.15143E-03	0.00000E+00
46	0.00000E+00	-3.50123E-03	0.00000E+00
47	0.00000E+00	-4.47113E-03	0.00000E+00
48	0.00000E+00	4.59017E-03	0.00000E+00
49	0.00000E+00	7.44108E-03	0.00000E+00
50	0.00000E+00	1.08673E-02	0.00000E+00
51	0.00000E+00	1.72570E-02	0.00000E+00
52	-7.28247E-04	1.01411E-03	1.23323E-03

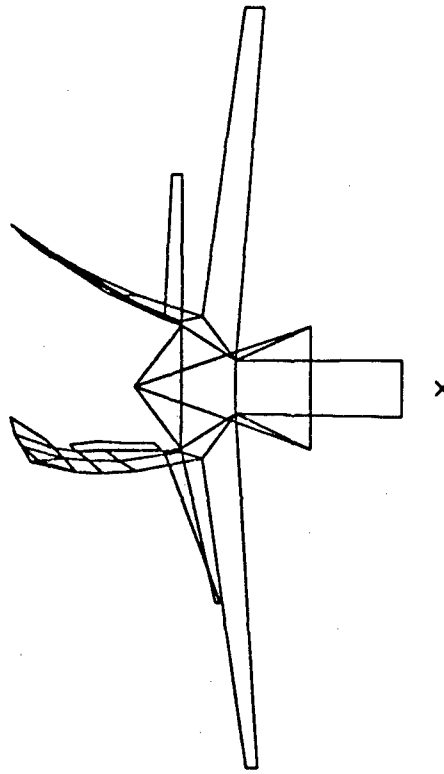
Table 22. 62.23 Hz, 45.5° AOA, Symmetric Mode Shape Listing

LOC	X	Y	Z
1	0.00000E+00	-1.09430E-03	0.00000E+00
2	0.00000E+00	-7.67586E-04	0.00000E+00
3	0.00000E+00	4.70830E-03	0.00000E+00
4	0.00000E+00	-4.96365E-03	0.00000E+00
5	0.00000E+00	-5.37401E-02	0.00000E+00
6	0.00000E+00	-3.33570E-02	0.00000E+00
7	0.00000E+00	-1.78153E-03	0.00000E+00
8	0.00000E+00	8.23202E-03	0.00000E+00
9	0.00000E+00	2.63373E-02	0.00000E+00
10	0.00000E+00	2.12614E-02	0.00000E+00
11	0.00000E+00	-9.74193E-03	0.00000E+00
12	0.00000E+00	-1.02726E-03	0.00000E+00
13	0.00000E+00	1.08413E-02	0.00000E+00
14	0.00000E+00	3.35638E-02	0.00000E+00
15	0.00000E+00	3.29580E-02	0.00000E+00
16	0.00000E+00	1.09566E-02	0.00000E+00
17	0.00000E+00	-2.87936E-03	0.00000E+00
18	0.00000E+00	3.55478E-03	0.00000E+00
19	0.00000E+00	1.86998E-02	0.00000E+00
20	0.00000E+00	2.63169E-02	0.00000E+00
21	0.00000E+00	-2.93555E-02	0.00000E+00
22	0.00000E+00	-5.65057E-02	0.00000E+00
23	0.00000E+00	-5.83403E-02	0.00000E+00
24	0.00000E+00	-7.47804E-02	0.00000E+00
25	-5.04801E-03	-1.15612E-02	-7.07171E-03
28	0.00000E+00	-1.34073E-03	0.00000E+00
29	0.00000E+00	-1.14825E-03	0.00000E+00
30	0.00000E+00	6.76220E-04	0.00000E+00
31	0.00000E+00	-3.67047E-03	0.00000E+00
32	0.00000E+00	-2.75339E-02	0.00000E+00
33	0.00000E+00	-1.18758E-02	0.00000E+00
34	0.00000E+00	-3.06049E-03	0.00000E+00
35	0.00000E+00	2.35577E-03	0.00000E+00
36	0.00000E+00	1.31979E-02	0.00000E+00
37	0.00000E+00	1.20746E-02	0.00000E+00
38	0.00000E+00	9.64393E-03	0.00000E+00
39	0.00000E+00	-2.31443E-03	0.00000E+00
40	0.00000E+00	4.21871E-03	0.00000E+00
41	0.00000E+00	1.64381E-02	0.00000E+00
42	0.00000E+00	1.81047E-02	0.00000E+00
43	0.00000E+00	2.30001E-02	0.00000E+00
44	0.00000E+00	4.69485E-04	0.00000E+00
45	0.00000E+00	4.15152E-03	0.00000E+00
46	0.00000E+00	6.31241E-03	0.00000E+00
47	0.00000E+00	5.69084E-03	0.00000E+00
48	0.00000E+00	-1.58002E-03	0.00000E+00
49	0.00000E+00	-1.34938E-02	0.00000E+00
50	0.00000E+00	-3.12782E-02	0.00000E+00
51	0.00000E+00	-4.89778E-02	0.00000E+00
52	-1.25283E-02	-2.58227E-03	1.36788E-03

Table 23. 63.57 Hz, 45.5° AOA, Antisymmetric Mode Shape Listing



Symmetric



Antisymmetric



Figure 17. Mode Shapes for Vertical Tail First Bending at 28.8° Angle of Attack

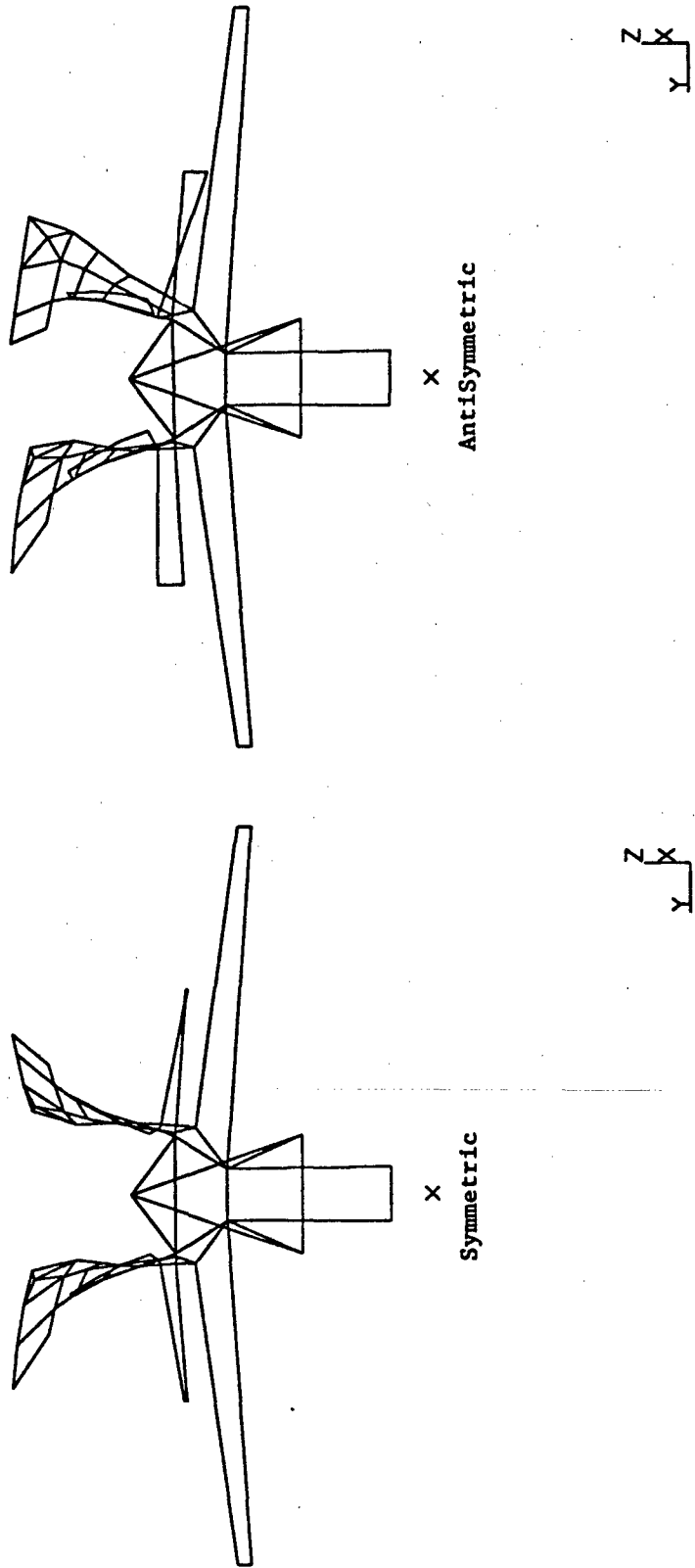
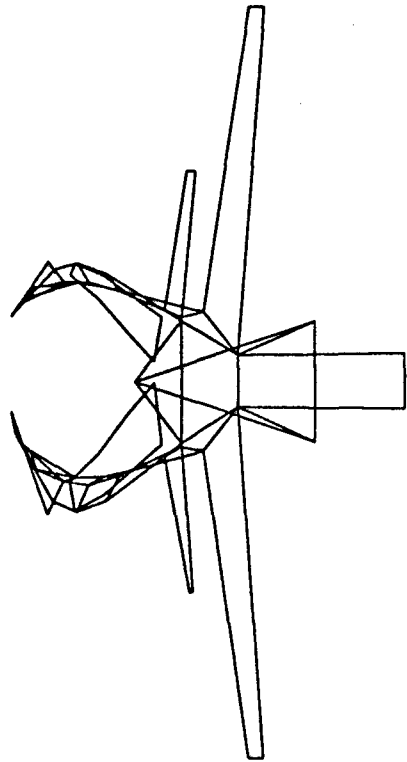
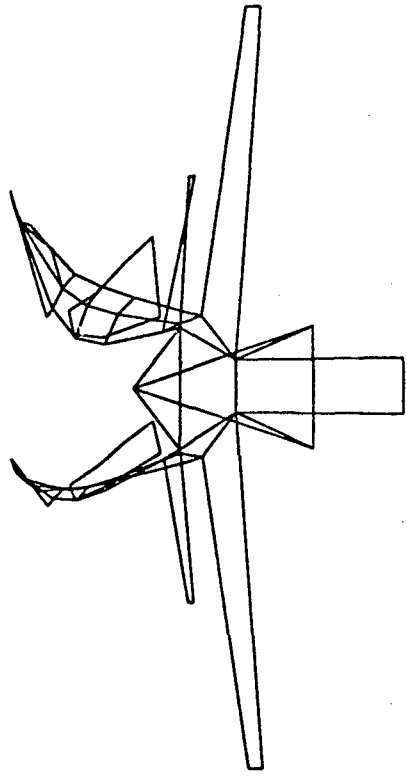


Figure 18. Mode Shapes for Vertical Tail First Torsion at 28.8° Angle of Attack



X
Symmetric



X
Antisymmetric



Figure 19. Mode Shapes for Vertical Tail Second Bending at 28.8° Angle of Attack

VI. CONCLUSIONS

A ground vibration test was conducted on a full-scale F-18 airframe mounted on the tunnel pedestals in the NASA Ames 80 ft x 120 ft wind tunnel facility. The F-18 airframe was significantly modified to prepare it for use as a wind tunnel model. The emphasis of the test was to determine the dynamics response characteristics of the vertical tails.

Nine test conditions were analyzed initially to determine the modal effects of adding bungees to restrict rudder motion, hydraulically powering the horizontal stabilators and changing the model angle of attack. Based on the test results neither the addition of bungee or hydraulic power affected the modal response of the vertical tail. In most cases, the change in modal frequency was less than 1.0%. In the case of the second bending modes, the changes reached 7.5%. It was concluded that the reason for such a high variation was because the shaker location did not excite that mode very well. The test data did show that the modal response was affected by the change in angle of attack. This was especially the case with the model support mode which saw a 12.8% change in frequency. The first and second bending modes changed at most 3.2% and 5.2% respectively indicating that the angle of attack played a significant role in changing the modal frequencies.

A detailed modal analysis was conducted on data for the 16.0°, 28.8° and 45.5° angle of attacks. All of the data were sampled for the model test conditions without the rudder bungees and with hydraulic power on. The detailed modal analysis successfully identified six model modal parameters including modal frequencies, damping ratios, and mode shapes for the symmetric and antisymmetric modes. The results were validated by comparisons with a previous ground vibration test and calculation of modal assurance criteria. The

vertical tail modes were generally found to be orthogonal.

The damping ratios were consistent with those found from the Canadian ground vibration survey for most test conditions. However, the damping ratio for the second symmetric bending mode of the 45.0° angle of attack was unreasonably low, in contrast to the Canadian results. The PolyreferenceTM method had some trouble estimating this mode; the difficulty may be related to the shaker location used for the test. Use of this estimated mode may be suspect but it is the best estimate obtained to date.

REFERENCES

1. Allemang, Randall J., Brown, David L., **Experimental Modal Analysis and Dynamic Component Synthesis, Volumes I-VI, AFWAL-TR-87-3069, December 1987.**
2. Ewins, D.J., **Modal Testing: Theory and Practice, New York, John Wiley, 1984.**
3. Henderson, Douglas A., Pacia, Arnel B, et al., **"C-18 Milstar Radome Modal Survey", AFWAL-TM-88-208-FIBG, November 1988.**
4. Lee, B.H.K., Brown, D., Zgela, M., and Poirel, D., **"Wind Tunnel Investigation and Flight Tests of Tail Luffet on the CF-18 Aircraft", AGARD Specialists' Meeting, Sorrento, Italy, 1-6 April, 1990.**
5. Meirovitch, Leonard, **Analysis Methods In Vibration, New York, The Macmillan Company, 1967.**

END

FILMED

DATE:

4-93

DTIC